Journal of Building Engineering 54 (2022) 104645

Contents lists available at ScienceDirect

Journal of Building Engineering

journal homepage: www.elsevier.com/locate/jobe

Selection of the optimal diagrid patterns in tall buildings within a multi-response framework: Application of the desirability function

Domenico Scaramozzino [a,*], Bonierose Albitos [a], Giuseppe Lacidogna [a], Alberto Carpinteri [a,b]

[a] Department of Structural, Geotechnical and Building Engineering, Politecnico di Torino, Corso Duca degli Abruzzi 24, 10129, Torino, Italy
[b] Department of Civil and Environmental Engineering, Shantou University, Shantou, China

ARTICLE INFO

Keywords:
Diagrid
Tall buildings
Matrix-based method
Desirability function
Multi-response optimization
Complexity index

ABSTRACT

Diagrids are efficient structural systems for tall building design and construction due to their high lateral stiffness. Their structural response can be optimized by changing the geometrical pattern of external diagonals. This has usually been carried out by looking for the diagonal pattern that employs the minimum amount of structural material, while complying with strength and stiffness requirements. However, other responses can be significant for the selection of the optimal pattern, such as the torsional flexibility and construction complexity of the building. In this work, the desirability function approach has been used for selecting the optimal diagonal pattern for diagrid tall buildings in a multi-response framework. The most desirable diagonal layout has been selected based on its overall desirability to minimize: (i) the wind-induced lateral displacement, (ii) the torsional rotation, (iii) the diagrid structural weight, and (iv) the construction complexity. The application of this methodology straightforwardly provides the optimal diagrid pattern considering the four responses simultaneously. The method has been applied initially to a limited set of uniform-angle patterns, and afterwards to a wider population of varying-angle geometries. Four different floor plan shapes were also taken into account. The outcomes of the analysis revealed that the specific plan shape plays only a minor role in the definition of the optimal structure, whereas the diagonal layout affects greatly the efficiency of the solution. Uniform-angle diagrids are generally the most desirable, even for taller buildings, due to their higher performance in terms of torsional rigidity and construction complexity. Among these, the patterns in which the diagrid triangular module spans over two-three floors, corresponding to diagonal inclinations of about 55°–65°, have the highest desirability. Notably, because of the competition between the different responses, this optimal inclination is not found to increase as the building becomes taller.

1. Introduction

Tall buildings emerged at the end of the 19th century in the United States, and then rapidly started to be realized in the 20th and then in the 21st century all over the world, as a possible solution to avoid horizontally overcrowded cities and excessive land consumption by conquering vertical space [1]. From a structural viewpoint, tall buildings need to withstand the massive vertical actions arising from gravitational dead and live loads. As the building becomes taller, there is also a "premium for height" to be paid due to the increasingly

* Corresponding author.
E-mail address: domenico.scaramozzino@polito.it (D. Scaramozzino).

https://doi.org/10.1016/j.jobe.2022.104645
Received 19 January 2022; Received in revised form 27 April 2022; Accepted 9 May 2022
Available online 13 May 2022

higher effects of lateral loads, which need to be counteracted by properly designed structural systems [2,3]. Examples of systems commonly employed in the interiors of the building are rigid and braced frames, shear walls, wall-frame systems, core-outrigger systems, etc., whereas examples of structural systems found in the external surface of the building include framed, braced, or bundled tubes, grid or tube-in-tube systems, super-frames, etc. [3].

A great deal of research is carried out nowadays aimed at proposing novel structural systems to improve the behavior of tall buildings against lateral actions. Wang et al. [4] recently proposed an adaptive negative-stiffness damped outrigger for a steel braced-core-tube framed-outrigger structure, achieving substantial damping effect in the elastic stage and guaranteeing the integrity of the building under excessive earthquake actions. Cao et al. [5] investigated the shear behavior of corrugated steel plate shear walls with inelastic buckling under lateral loads, suggesting that these have the potential to withstand lateral actions in tall buildings. Li et al. [6] carried out experimental and numerical analyses to assess the seismic performance of L-shaped double-steel plate shear walls. Buckling-restrained steel plate shear walls were recently proposed by Tan et al. [7] and Wang et al. [8], whose performance under cyclic loading can be beneficial in high-rise buildings. Labrecque et al. [9] explored the use of prefabricated light-frame sub-structures for tall building design and construction. Abundant research is also being carried out regarding new design and optimization procedures for the improvement of tall building behavior, while limiting material usage. For instance, Amoussou et al. [10] proposed novel performance-based design procedures for outrigger and ladder tall building models under seismic scenarios. Wang and Tsavdaridis [11] recently explored the applicability of an optimality criteria-based minimum-weight design method for modular building systems, which aims at reducing their self-weight while maintaining their lateral stiffness. Xu et al. [12] carried out an optimal design of supertall buildings based on high-frequency force balance wind tunnel experiments.

One of the main structural systems that captured a great attention within the tall building research community and structural engineering companies is, without doubts, the diagrid. Diagrids are amongst the most attractive structural systems for tall buildings, due to their high lateral stiffness and remarkable architectural appearance [13–15]. They exploit the axial deformation of diagonals, arranged in triangular patterns over the external surface of the building, to withstand both lateral and vertical actions [16–18]. The diagonals act both as bracings and vertical resisting elements, providing the diagrid a competitive structural efficiency for buildings up to 100–130 stories [2,3].

Other than providing high stiffness against lateral actions, the main deformation mode of the structure – which is based on the axial shortening-elongation of the diagonals – has enabled various researchers to develop simplified methodologies for the preliminary design. Moon et al. [19] proposed a method for the stiffness-based preliminary design of rectangular uniform-angle diagrids. A similar approach was subsequently developed for varying-angle patterns [20], and patterns with curved diagonals [21]. Both stiffness and strength criteria were taken into account by Mele et al. [22,23], where it was shown that the slenderness of the building plays a major role in defining the preliminary design. Slender diagrids are more sensible to stiffness-based requirements, while strength-based criteria should be used for the design of buildings with lower aspect ratio [24]. More recently, a stiffness-based preliminary methodology was also developed for twisted diagrids [25].

Based on the main assumptions of these methodologies for the preliminary design, i.e., (i) the diagrid is the main structural system withstanding lateral loads, (ii) the diagonals carry only axial force with linear elastic behavior, (iii) the floors remain plane after the deformation, various simplified approaches were also developed for the structural analysis of the diagrids. Liu and Ma [26] developed the modular method (MM), where an arbitrary polygonal diagrid tube was divided into stacked modules. Shear and bending stiffness of these modules were analytically evaluated based on geometric and static considerations, providing simple equations to calculate the lateral displacements under lateral loads [26]. Shi and Zhang [27] proposed to model the diagrid tube as an equivalent elastic orthotropic membrane. Based on the equivalence of the lateral displacements, the elastic and shear modulus of the equivalent membrane were computed, eventually leading to the calculation of displacements and internal stresses. This approach also provided a simplified way to evaluate the shear-lag effect [27]. Recently, a matrix-based method (MBM) was developed by us, which is based on the direct computation of the diagrid stiffness matrix, enabling to perform the structural analysis under lateral, vertical and torque actions [28]. The method allows to compute the displacements and rotations of the building floors, as well as the axial forces in the diagonals, under general loading conditions for generic free-form diagrids. The MBM was subsequently applied to study the influence of the diagrid geometry on the structural response under both lateral and torque actions [29], also considering the presence of closed- or open-section shear walls [30,31].

One of the main features that led the diagrid to become extremely attractive in the design and construction of tall buildings is its ability to achieve optimized structural responses through geometric modifications of the diagonal pattern. Moon et al. [19] first showed that there exists a diagonal inclination that minimizes the weight of the structure while complying with strength and stiffness requirements. Diagonals with inclination of about 35° are optimal to withstand shear, while inclinations of 90° are ideal to carry overturning moments. Thus, the optimal inclination lies in between these values, often in the range 65°–75°. The optimal value depends on the competition between bending and shear actions. In slender buildings, bending moments prevail, therefore higher values of the optimal angle are expected. In shorter buildings, shear actions prevail, thus shallower diagonals are more beneficial for the limitation of lateral displacements [19]. Since bending also prevails at the bottom of the building, while shear actions prevail at the top, varying-angle diagrid patterns were also proposed. In these patterns, steep diagonals are employed at the bottom of the building, while shallow diagonals are placed at the top [20,21,32]. Additional patterns were suggested afterwards, such as variable-density patterns [33,34], layouts inspired to the principal stress lines [35,36], and configurations based on topological optimization [37–39]. Some studies also focused the attention on the influence of the floor shape on the diagrid structural response [29,40,41].

The majority of research works mentioned above generally selected the optimal geometry as the one employing the least amount of structural material and leading to the lowest lateral displacements, while complying with all strength requirements under vertical and lateral loads [33–41]. However, other than the weight and lateral flexibility, other variables can affect the suitability of a certain

diagrid solution. The torsional flexibility of the building under eccentric loads should be minimized, to avoid serviceability issues [29, 30]. The construction complexity of the structure should also be limited, in order for the building to be feasible from a constructability perspective [35,39]. For this purpose, a complexity index (*CI*) was proposed by Tomei et al. [35], to quantify the complexity of the diagonal pattern depending on its geometric parameters. As a result, if the optimal diagrid geometry must be selected to minimize multiple variables, e.g., structural weight, lateral displacements, torsional flexibility, and construction complexity, a multi-response optimization framework is needed. The desirability function approach can be used for this purpose [42].

The desirability function was firstly proposed by Harrington [43], and then adapted by Derringer and Suich [44], to tackle multi-response optimization problems. This approach is based on the assignment of desirability scores, between 0 and 1, based on the comparison of the performance of all the solutions within a certain population. Individual desirability values are first assigned based on the performance of each solution with respect to each response. Then, these individual desirability values are combined to obtain a unique value of the overall desirability, which considers the overall suitability, i.e., desirability, of each solution with respect to all the responses. The most desirable solution is then simply selected as the one with the highest value of overall desirability.

Recently, we made use of the desirability function for the evaluation of the optimal diagrid geometry [45]. A set of uniform-angle diagrid structures, with different diagonal inclinations and floor plan shapes, was investigated under lateral and torque actions. The lateral displacements due to the lateral loads, the torsional rotation due to the torque actions, the total weight of the diagrid, and the construction complexity of the building were all considered within the multi-response framework of the desirability function [45]. Based on the results, we were able to select the optimal diagrid pattern. However, in [45] the performance of the buildings was only assessed under lateral and torque actions, and the cross-sectional areas of the diagonals were kept the same amongst all geometric solutions, therefore the stress conditions of the diagonals were not optimized in terms of the demand-to-capacity ratio (DCR). Moreover, only uniform-angle diagrid patterns and lateral actions were considered in [45]. Here, the desirability function approach is applied for the multi-response optimization of both uniform- and varying-angle diagrid structures under lateral, vertical and torque actions, while also considering the optimization of the diagonal DCRs in the preliminary design stage. This will provide a more realistic and comprehensive assessment of the optimal diagrid pattern.

2. Structural analysis, diagrid geometries and desirability function

2.1. Matrix-based method (MBM), loading conditions and structural analysis

In this work, we made use of the matrix-based method (MBM) for the structural analysis of uniform- and varying-angle diagrid geometries. This method has been developed within the MatLab environment, and the code is available in the Supplementary Material as a MatLab function. As briefly mentioned in the Introduction, the MBM allows to perform the structural analysis of diagrids under both lateral, vertical and torque actions [28]. Lateral and torque actions arise from the wind pressure acting on the building surface, while vertical actions come from the dead and live loads acting on the floor slabs.

Dead and live loads were assumed to be 7 kN/m^2 and 4 kN/m^2, respectively. Following Montuori et al. [22], we assumed that the central core occupies 25% of the building floor area. Thus, the core absorbs the 72.5% of the gravity load (25% of the occupied area, plus half of the remaining 75%), while the external diagrid absorbs the remaining 37.5%. These vertical uniform loads acting on the external diagrid were then converted into vertical point forces acting at the level of floor centroids and included into the MBM for the structural analysis.

The contribution of the central core to the lateral loads was neglected, therefore it was assumed that the diagrid absorbs 100% of the load arising from the wind pressure. Wind actions were evaluated from ASCE 7–10 [46], assuming the building is located in New York and the basic wind speed is equal to 40 m/s. The obtained wind pressure was then converted into floor forces and torque moments (for the torque moments, we used the suggested eccentricity value of 15% [46]). The values of these actions were finally inserted into the MBM, to evaluate the lateral deflection of the building and the torsional rotations of the floors.

The axial loads in the diagonals arising from the vertical, lateral and torque actions were also evaluated by the MBM. Circular-hollow sections (CHSs) were used for the diagonals, which are made of steel, with a mass density of 7.8 ton/m^3, elastic modulus of 210 GPa, and yield stress of 275 MPa. Table S1 in the Supplementary Material reports the complete list of 176 CHSs considered, taken from [47]. Twenty-four diagonals were placed within each diagrid module. Strength conditions were assessed by comparing the axial load and the diagonal resistance. Tensile resistance was used for tensed members, while buckling resistance was calculated for compressed members. The demand-to-capacity ratio (DCR) was finally computed as the ratio between the acting axial load and the member resistance.

The values of the cross-sectional areas of the diagonals were then assigned to satisfy both strength and stiffness criteria. Each diagrid geometry was initially analyzed under vertical, lateral and torque actions by assigning tentative values of these cross-sectional areas. The DCR for all diagonals and the total lateral displacement at the top of the building, δ_{top}, were calculated via the MBM. Then, the cross-sectional areas of the CHS diagonals at the different modules were modified until strength and stiffness criteria were met, i.e., DCR <1 for all diagonals and $\delta_{top} < \delta_{lim}$. Here, δ_{lim} represents the maximum allowable deflection of the building due to lateral loads, which is commonly assumed as $H/500$, H being the total height of the building. The cross-sectional areas leading to a satisfying diagrid solution, both in terms of strength and stiffness, were then kept for subsequent analysis and for comparison among the different diagrid geometries. The MatLab codes for evaluation of diagonal strength, calculation of DCR, and building preliminary design can also be found in the Supplementary Material.

2.2. Diagrid geometries

Four different floor shapes and building aspect ratios were considered for both uniform- and varying-angle diagrids. Square,

hexagonal, octagonal, and circular buildings were analyzed, as shown in Fig. 1a [29,45]. The floor dimensions were set up in order to have a gross floor area equal to 900 m^2, leading to an average footprint of the building of 30 m × 30 m (Fig. 1a). Fig. 1b shows the four heights, i.e., 126, 168, 210, and 252 m. The inter-story height of all buildings is equal to 3.5 m. Thus, the total number of floors N associated to the four building heights are 36, 48, 60, and 72. The aspect ratios of the four buildings are then 4.2, 5.6, 7.0, and 8.4, respectively.

2.2.1. Uniform-angle diagrids

For each floor plan shape and aspect ratio shown in Fig. 1, six different uniform-angle diagrid patterns were generated by varying the number of floors included within each diagrid module, $n_{f,m}$, with $n_{f,m}$ equal to 1, 2, 3, 4, 6, and 12 (Fig. 2). Note that, in this work, consistently with the MBM framework [28], the diagrid module is defined by the height associated to the single diagrid triangle. The different diagrid patterns with varying $n_{f,m}$ are associated with different inclinations of the diagonals, with angles ranging from about 35° (for $n_{f,m} = 1$) up to about 84° (for $n_{f,m} = 12$) [29,45].

2.2.2. Varying-angle diagrids

It is known that bending and shear actions affect the design of different portions of the tall building in a different way. At the top of the building shear prevails over bending moment, whereas bending actions prevail at the bottom. Furthermore, the higher the slenderness of the building, the higher the importance of bending with respect to shear. Table 1 reports the values of the total shear force, overturning moment, and torque moment at the base of each of the four buildings.

As can be seen, as the height of the building increases, the overturning moment increases much faster than the shear force. This is expected to have an impact on the design and behavior of the structure. We have mentioned above that steeper diagonals are more suitable to carry vertical loads and overturning moments, while shallower diagonals are optimal for withstanding shear [19]. As a result, it is reasonable to place steep diagonals at the base of the building, where the overturning moments and vertical loads prevail, and to place shallow diagonals at the top, where shear actions are prevailing [21]. This varying-angle configuration of diagonals is expected to optimize the structural behavior under lateral loads, as it is closer to the principal stress lines [36]. It is also expected that this configuration should be more efficient as the building height increases. However, these considerations take into account only the structural response of the building under lateral actions, but they do not consider how the varying-angle pattern influences the torsional flexibility of the structure or its construction complexity. To assess such influence, in this work we considered a wider range of diagrid solutions for the building geometries reported in Fig. 1, employing varying-angle patterns.

A large variety of varying-angle geometries was built for each of the four buildings and floor plan shapes. These diagonal patterns were generated by covering the building with diagrid modules having different numbers of intra-module floors j. All the possible combinations of diagrid modules, including a number of intra-module floors j equal to 1, 2, 3, 4, 5, and 6, were computed based on combinatorial calculus. Only the solutions able to cover exactly the N floors of the building were retained as feasible varying-angle solutions, i.e., only those solutions satisfying the following equation:

$$N = \sum_{j=1}^{6} jM_j, \tag{1}$$

where M_j is the total number of modules in the diagrid pattern with a number of intra-modules floors equal to j. As an example, for the building with $N = 48$, we obtained a total of 7760 feasible varying-angle patterns. Four of these varying-angle geometries for the building with $N = 48$ and square plan shape are shown in Fig. 3.

Considering the four different floor shapes reported in Fig. 1a, for the 48-floor building we obtain a complete population of 31040 varying-angle patterns. The total number of patterns for the buildings with $N = 36$, 60, and 72 are 9728, 79432, and 175008, respectively. Only those solutions with steeper diagonals at the bottom and shallower at the top were considered, since the opposites

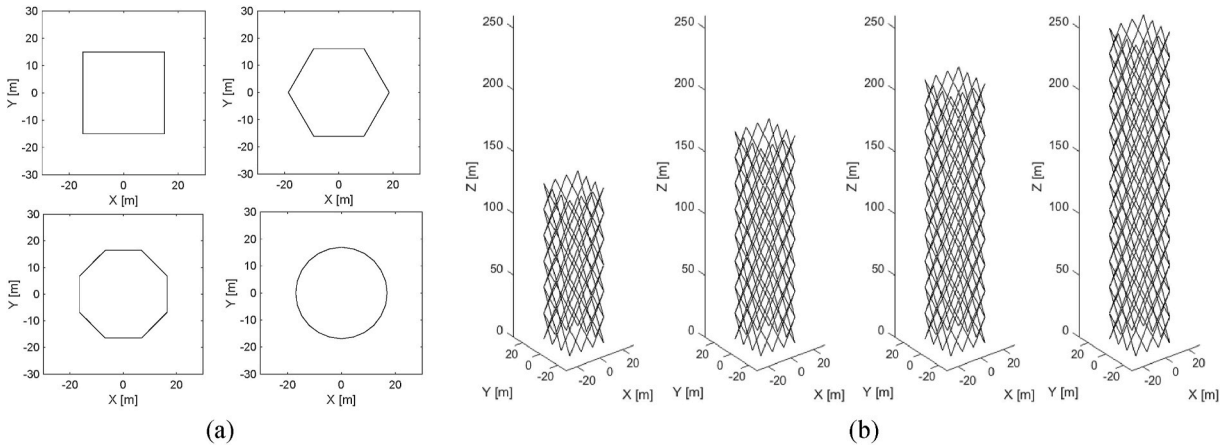

Fig. 1. Diagrid geometries: (a) floor plan shapes (square, hexagonal, octagonal, and circular), and (b) building heights (only shown for the square plan shape).

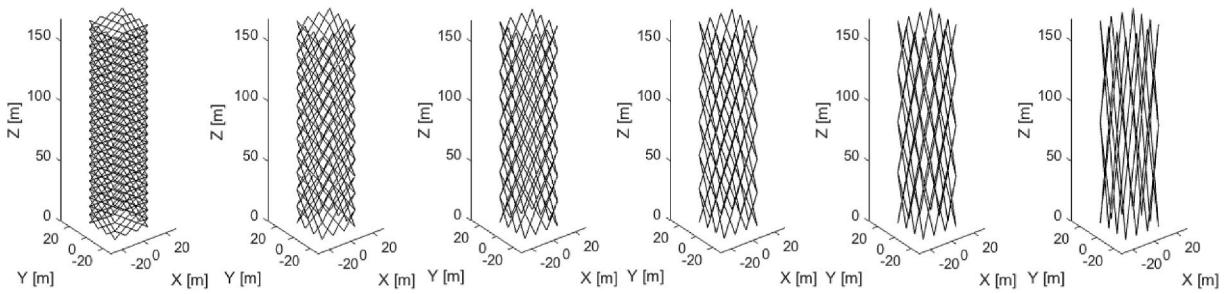

Fig. 2. Uniform-angle diagrid pattern with $n_{f,m} = 1$, 2, 3, 4, 6, and 12 (here only the diagrid patterns with the square floor shape and for the 48-floor building are shown for brevity).

Table 1
Total shear, overturning moment, and torque moment at the base of each building due to lateral wind load.

H [m]	126	168	210	252
Total shear force [MN]	7	10	14	18
Total overturning moment [MNm]	447	887	1518	2363
Total torque moment [MNm]	30	44	61	79

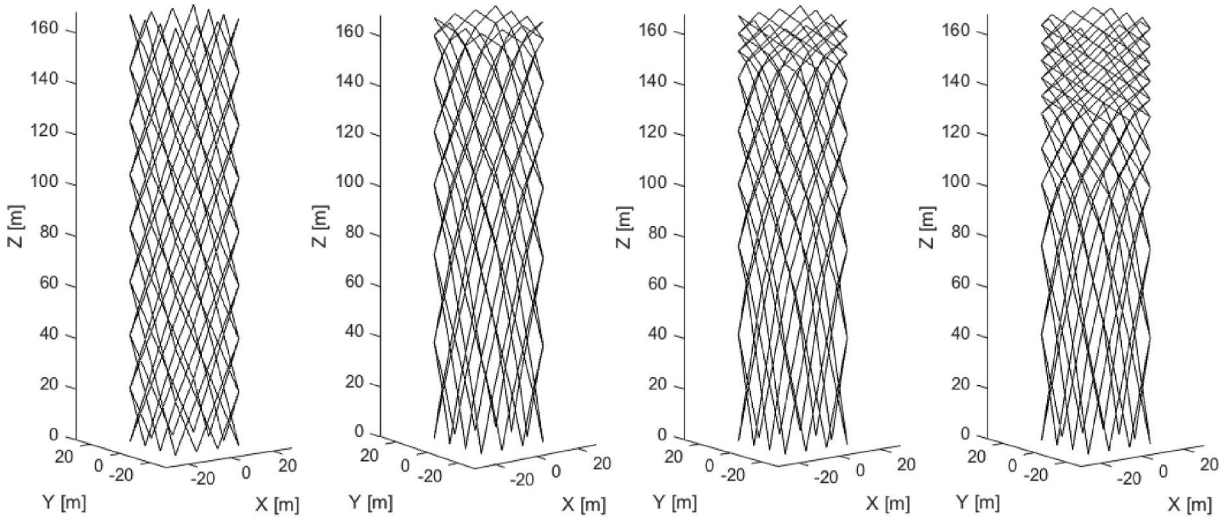

Fig. 3. Four examples, out of the 7760, of varying-angle diagrid patterns for the square 48-floor building. Each pattern can be identified with the set of M_j values, M_j being the number of diagrid modules containing j intra-module floors, with $j = 1, 2, \ldots, 6$. In this figure, from left to right: (i) pattern #88, $M_1 = M_2 = M_4 = M_5 = M_6 = 0$, $M_3 = 16$ (note that this is the uniform-angle diagrid with $n_{f,m} = 3$); (ii) pattern #1373: $M_1 = 2$, $M_2 = 1$, $M_3 = 5$, $M_4 = 2$, $M_5 = 3$, $M_6 = 1$; (iii) pattern #2928: $M_1 = 5$, $M_2 = 1$, $M_3 = 5$, $M_4 = 2$, $M_5 = 0$, $M_6 = 3$; and (iv) pattern #5209: $M_1 = 11$, $M_2 = 4$, $M_3 = M_4 = 1$, $M_5 = M_6 = 2$.

(shallow diagonals at the bottom and steep at the top) behave against structural logic [48]. Also note that, within the population of the thousands varying-angle patterns generated in this way, the smaller population of uniform-angle diagrids (Fig. 2) is also included. These are the ones having $M_j = 0$ for all values of j, except for $j = n_{f,m}$, which is the number of intra-module floors representative of the uniform-angle diagrid (see Fig. 3, first panel at the left).

2.3. Desirability function approach

The desirability function approach can be used to assess the best, i.e., most desirable, solution within a certain population in order to satisfy certain conditions [42–44]. It is a simple yet very efficient methodology, especially when there is the need to select the best solution in a multi-response framework. In tall building design, the optimal diagrid solution has usually been selected as the one with the minimum weight, while satisfying strength and stiffness requirements [19,22,33,48]. However, different diagrid geometries can have profoundly different behaviors in terms of torsional flexibility [29,30,45], and construction complexity [35,39,45]. As a result, the lightest diagrid geometry complying with the maximum allowable lateral displacement might be too much deformable under torque actions or it might be too much complex from a construction point of view. For this reason, the selection of the optimal diagrid geometry needs to be addressed in a multi-response framework, where lateral deflections, structural weight, torsional flexibility, and

construction complexity need to be considered simultaneously. The desirability function approach provides a simple, fast, and efficient methodology to tackle this problem [45].

The approach is based on the evaluation of the individual desirability of each solution i with respect to a certain response p, $d_{i,p}$, and the combination of these individual desirability values into an overall desirability score for each solution i, OD_i. In this study, the solution i refers to each diagrid pattern. The response p refers to the selected response, i.e., top lateral displacement under wind actions ($p = \delta_{i,top}$), total weight of the diagrid system ($p = W_i$), top torsional rotation due to the eccentric wind action ($p = \varphi_{i,top}$), and construction complexity measured via the complexity index ($p = CI_i$).

The top lateral displacement under wind actions, $\delta_{i,top}$, as well the top torsional rotation due to the eccentric wind action, $\varphi_{i,top}$, were calculated via the MBM, as explained in Section 2.1. Note that, if the stiffness-based criteria rule the preliminary design, the top displacement meets exactly the maximum lateral deflection, i.e., $\delta_{i,top} = \delta_{lim} = H/500$. Conversely, if strength-based criteria prevail, the lateral deflection of the building turns out to be lower than δ_{lim}, i.e., $\delta_{i,top} < \delta_{lim}$. The total weight of the diagrid system, W_i, was simply calculated based on the total mass of diagonals, depending on their geometric (cross-sectional area and length) and material (mass density) properties. Finally, the complexity index, CI_i, was calculated for each structure as proposed by Tomei et al. [35].

The complexity index puts five construction parameters (N_1, N_2, N_3, N_4, N_5) together, that depend on the geometric features of the pattern. N_1 is the weighted number of nodes in the pattern, i.e., the number of joints in the pattern multiplied by a parameter considering the joint connectivity. N_2 represents the total number of different cross-sections used in the pattern. N_3 is the number of splices required for the diagonals in the pattern, assuming a maximum length of 12 m for transportation. N_4 represents the total number of diagonals in the pattern. N_5 is the number of different lengths of all diagonal members. Once these five parameters were calculated for each diagrid geometry i, they were normalized to the maximum value across the population, and the sum of these five normalized parameters finally gave the complexity index for each diagrid solution i [35]:

$$CI_i = \sum_{k=1}^{5} \left(\frac{N_{k,i}}{\max_i N_{k,i}} \right), \tag{2}$$

As a result, the complexity index can have values between 0 and 5 for each diagrid solution. Higher values of CI imply higher construction complexity.

Once the four responses were calculated for each diagrid solution i, i.e., $\delta_{i,top}$, $\varphi_{i,top}$, W_i, and CI_i, the desirability function approach was used to assign an individual desirability score to each solution i for each response p. Since the most desirable diagrid solution is the one leading to the minimum value of each response, the individual desirability value can be written in general form as [42,44]:

$$d_{i,p} = \left(\frac{U_p - p_i}{U_p - L_p} \right)^{r_p}, \tag{3}$$

where U_p and L_p represent the upper and lower bounds for response p, and r_p is an exponent defining the amount of desirability of the solution within the range $L_p – U_p$. The upper and lower bounds can be defined independently for each response variable p. The exponent r_p can assume the same value or different values for each response p, depending on whether the designer wants to assign a higher weight to a certain response. Higher values of r_p are associated with a higher impact of the response p in the optimization process [42, 44,45]. In this work, the value of r_p was set equal to 1 for all four responses, i.e., $\delta_{i,top}$, $\varphi_{i,top}$, W_i, and CI_i. A different choice can obviously be made by the designer, by changing the r_p values for each response, depending on the different weight each response should have in the optimization process.

To calculate the individual desirability values for the four considered responses, Equation (3) was adjusted for each response as follows:

- As regards the torsional rotation $\varphi_{i,top}$, since design codes do not provide maximum allowable values of torsional rotations, the upper bound U_φ was simply defined as the maximum rotation achieved within the population. Conversely, the lower bound L_φ was set to 0, which represents the lowest value that this response could theoretically achieve. Therefore, the formulation for $d_{i,\varphi}$ turns out to be:

$$d_{i,\varphi} = \left(\frac{\max_i \varphi_{i,top} - \varphi_{i,top}}{\max_i \varphi_{i,top}} \right)^{r_\varphi} = \left(1 - \frac{\varphi_{i,top}}{\max_i \varphi_{i,top}} \right)^{r_\varphi}. \tag{4}$$

In this way, the diagrid pattern with the highest torsional rotation within a certain population has a value of $d_{i,\varphi}$ equal to 0, whereas the ones with lower values of $\varphi_{i,top}$ have values of $d_{i,\varphi}$ gradually approaching to 1. The more $\varphi_{i,top}$ is close to 0, the more the building is torsionally stiff, and the more $d_{i,\varphi}$ is then close to 1. The exponent r_φ modulates the variation of $d_{i,\varphi}$ values in this range. As mentioned above, here r_φ was simply set equal to 1.

- Similarly, the upper and lower bounds associated to the diagrid weight W_i, i.e., U_W and L_W, were set to the maximum value achieved within the population and 0, respectively:

$$d_{i,W} = \left(\frac{\max_i W_i - W_i}{\max_i W_i} \right)^{r_W} = \left(1 - \frac{W_i}{\max_i W_i} \right)^{r_W}. \tag{5}$$

Therefore, the heaviest structure in the population has a value of $d_{i,W}$ equal to 0, whereas lighter solutions have values of $d_{i,W}$ gradually approaching to 1. The lower W_i, the lighter the diagrid system, the closer $d_{i,W}$ to 1. Again, the exponent r_W modulates the values of $d_{i,W}$ in this range, and was set equal to 1 in this work.

- The upper and lower bounds related to the complexity index CI_i, i.e., U_{CI} and L_{CI}, were set equal to 5 and 0, respectively. As a matter of fact, these represent the highest and lowest values that the CI can attain according to Equation (2). The mathematical formulation for $d_{i,CI}$ turns out to be:

$$d_{i,CI} = \left(\frac{5 - CI_i}{5}\right)^{r_{CI}} = \left(1 - \frac{CI_i}{5}\right)^{r_{CI}}. \tag{6}$$

Since generally no solution has a complexity index of 5 or 0, all solutions will exhibit values of $d_{i,CI}$ between 0 and 1. The lower CI_i, the less complex the structure, the closer $d_{i,CI}$ to 1. Again, the exponent r_{CI} modulates the variation of $d_{i,CI}$ values. Again, it was set equal to 1 here.

- For $\delta_{i,top}$, the definition of the individual desirability score $d_{i,\delta}$ is trickier, since $\delta_{i,top}$ is not just a response, but also a parameter that drives the preliminary design of the structure. As a matter of fact, three cases were observed after the preliminary design stages: (i) some diagrid solutions exhibited values of $\delta_{i,top}$ higher than δ_{lim}, because no CHS cross-sections, out of the 176 ones available in [47], were large enough to satisfy neither stiffness- nor strength-based constraints; (ii) all diagrid solutions within the analyzed population had the same value of $\delta_{i,top} = \delta_{lim}$, since the stiffness criteria governed the design for all diagrid patterns in the population; (iii) some diagrid solutions within the population presented values of $\delta_{i,top}$ lower than δ_{lim}, because their preliminary design was ruled by strength-based constraints. Case (i) was simply addressed by assigning a value of $d_{i,\delta} = 0$ to those diagrid solutions exceeding the maximum allowable lateral displacement, i.e.,:

$$\delta_{i,top} > \delta_{lim} \Rightarrow d_{i,\delta} = 0\,. \tag{7a}$$

As a matter of fact, these solutions are completely undesirable from a lateral flexibility perspective. On the other hand, case (ii) was addressed by assigning a unit value of individual desirability to all diagrid patterns in the population, i.e.:

$$\nexists i \in P \left| \delta_{i,top} < \delta_{lim} \right. \Rightarrow d_{i,\delta} = 1,\ \forall i \in P, \tag{7b}$$

where P denotes the population of uniform- or varying-angle diagrids. This condition occurs when all the diagrid solutions within the population are preliminary designed according to the stiffness requirements. In this case, the top lateral displacement of all solutions is the same, as it matches the limit value of δ_{lim}, and consequently all solutions turn out to have the same desirability value $d_{i,\delta}$. Finally, case (iii) was solved by considering the following equation for $d_{i,\delta}$:

$$\exists i \in P \left| \delta_{i,top} < \delta_{lim} \Rightarrow d_{i,\delta} = 0.5\left[1 + \left(1 - \frac{\delta_{i,top}}{\delta_{lim}}\right)^{r_\delta}\right]. \right. \tag{7c}$$

In this case, diagrid patterns can have different desirability scores $d_{i,\delta}$ depending on the values of the lateral displacement. According to Equation (7c), the solutions for which the lateral displacement $\delta_{i,top}$ is equal to the maximum allowable value δ_{lim}, which reflect a preliminary design ruled by stiffness conditions, have a value of $d_{i,\delta}$ equal to 0.5. Conversely, diagrid solutions for which $\delta_{i,top}$ is lower than δ_{lim}, which reflect a preliminary design ruled by strength requirements, have a value of $d_{i,\delta}$ higher than 0.5. The lower $\delta_{i,top}$ with respect to δ_{lim}, the higher $d_{i,\delta}$, in the range 0.5–1. Note that the difference between case (ii) and case (iii) is that in case (ii) all diagrid pattern within the population are designed according to stiffness criteria, therefore you have $\delta_{i,top} = \delta_{lim}$, and hence $d_{i,\delta} = 1$, for all patterns. On the other hand, in case (iii) you can have diagrid patterns whose design is ruled either by strength or stiffness requirements. As a result, you can find solutions with $\delta_{i,top} < \delta_{lim}$, for which an increase in the relative value of individual desirability score $d_{i,\delta}$ is provided by the application of Equation (7c).

Once all individual desirability scores were computed for each diagrid solution i and in relation to each response p according to Equations (4–(7), the overall desirability OD_i was computed as follows [42,44,45]:

$$OD_i = \prod_{p=1}^{4} \left(d_{i,p}\right)^{\frac{1}{4}} = \left(d_{i,\delta} \cdot d_{i,\varphi} \cdot d_{i,W} \cdot d_{i,CI}\right)^{\frac{1}{4}}. \tag{8}$$

As can be seen, Equation (8) allows to obtain a unique desirability score, between 0 and 1, for each diagrid solution i, considering simultaneously the performance of each diagonal pattern in terms of lateral and torsional flexibility, structural weight, and construction complexity. The solutions with the highest values of OD_i were finally selected as the most desirables.

3. Results and discussion

In this section, the results are reported which arose from the preliminary design based on stiffness- and strength-based criteria by means of the MBM (Section 2.1), and from the selection of the most desirable diagrid geometry based on the desirability function (Section 2.3). First, the results obtained for the limited set of twenty-four uniform-angle diagrid patterns are shown in Section 3.1, while the wider population of varying-angle geometries is investigated in Section 3.2.

3.1. Uniform-angle diagrids

As reported in Section 2.2.1, for each of the four buildings (36-, 48-, 60-, and 72-floor buildings shown in Fig. 1b), four plan shapes (Fig. 1a) and six uniform-angle diagrid patterns (Fig. 2) have been considered. This leads to a total of twenty-four uniform-angle diagrid solutions for each building. These solutions are labeled according to the specific plan shape (Fig. 1a) and number of intra-module floors (Fig. 2). For example, S4 stands for the square diagrid with $n_{f,m}$ equal to 4, C12 for the circular building with $n_{f,m}$ equal to 12, and so on. Each of these patterns has been analyzed via the MBM under vertical, lateral and torque loads. Proper diagonal cross-sections have been assigned to comply with strength and stiffness requirements (see Section 3.1.1). The desirability function has then been applied to select the most desirable uniform-angle solution simultaneously minimizing the lateral deflection, torsional rotation, diagrid weight, and construction complexity (see Section 3.1.2).

3.1.1. Preliminary member sizing

Based on the strength- and stiffness-based preliminary design under vertical, lateral and torque actions, Fig. 4 shows the maximum and minimum cross-sectional areas assigned to all diagrid patterns for all building heights. Maximum cross-sectional areas correspond to the ground modules, while minimum areas correspond to the top modules. The complete list of all cross-sections for each structure is reported in Tables S2–S17 in the Supplementary Material.

From this figure and the Supporting Tables, it can be observed that: (i) higher buildings require increasingly larger cross-sections, due to the rapidly increase in the external and internal loads; (ii) for a selected building and inclination of diagonals, similar cross-sections are adopted for different plan shapes, suggesting that the specific plan shape plays only a minor role in the preliminary design; (iii) for a selected building and floor plan shape, the cross-sections are larger for the minimum and maximum number of intra-module floors $n_{f,m}$, suggesting that a range of optimal diagonal inclinations exists which leads to the lightest cross-sections, i.e., to the lowest amount of structural weight W_i; (iv) some diagrid solutions are found to be so intrinsically flexible that no CHS members available in [47] are large enough to satisfy stiffness- and strength-based requirements. This is the case of pattern S1 for the 60-floor building, and patterns S1, H1, O1, C1, and C12 for the 72-floor building. As reported in Section 2.3, since these solutions are not able to satisfy the lateral displacement requirement (see Fig. 5 below), according to Equation (7a) they are assigned an individual desirability value $d_{i,\delta}$ of 0.

Fig. 5 reports the values of the lateral displacement at the top of the building under the effect of lateral wind pressure. These values are reported for each building height and depending on the specific diagonal pattern (S1, S2, …, C12).

The preliminary design of the shortest building ($N = 36$), with aspect ratio of 4.2, is mainly ruled by strength conditions, since almost none of the diagrid patterns meets exactly the target δ_{lim} of 0.25 m. Some of the solutions approach this value, but all of them have $\delta_{i,top} < \delta_{lim}$. The minimum displacement is obtained by pattern S3, with a top lateral displacement $\delta_{i,top}$ equal to 0.15 m, which is more than 40% lower than the maximum allowable for to the stiffness design. This is in accordance with the findings in [22,24], which confirmed that the preliminary design of diagrids is ruled by lateral displacement requirements generally for aspect ratios higher than 5. In shorter buildings, strength requirements are expected to drive the preliminary member sizing. Note that this population of diagrids is associated to case (iii) reported in Section 2.3 as regards the calculation of the individual desirability value $d_{i,\delta}$. For this reason, Equation (7c) will be applied for the computation of the individual desirability values $d_{i,\delta}$. The highest value of $d_{i,\delta}$ will be reached by pattern S3, as it exhibits the minimum value of the lateral displacement.

Conversely, in the building with 48 floors (aspect ratio of 5.6), all solutions reach the target displacement limit, $\delta_{lim} = 0.34$ m, thus suggesting that the stiffness requirements drive the preliminary design of all these patterns. Hence, this population is associated to case (ii) reported in Section 2.3 for the calculation of $d_{i,\delta}$. For this reason, all values of $d_{i,\delta}$ are set here equal to 1.

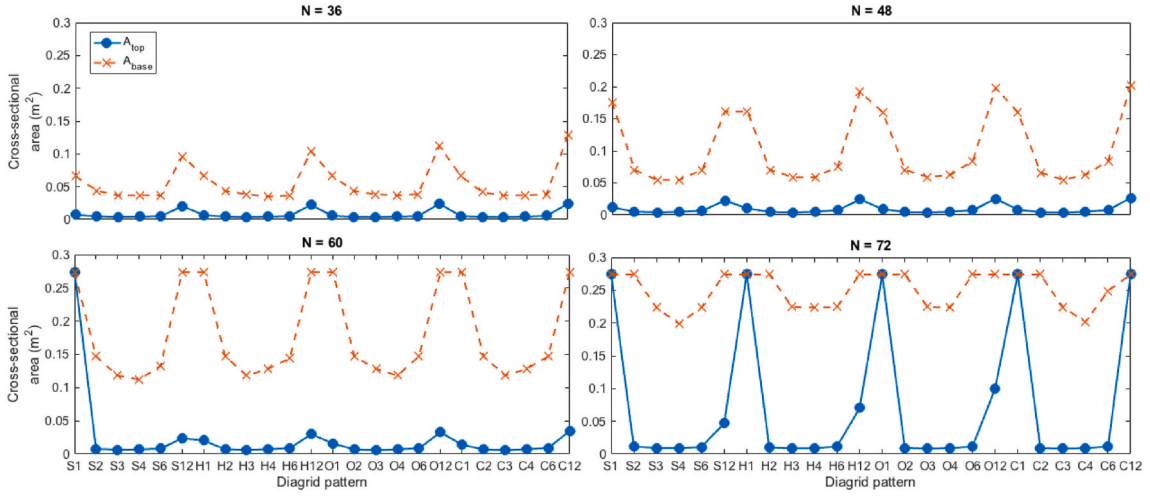

Fig. 4. Cross-sectional areas (in m^2) for the top (continuous blue line) and base (dashed orange line) modules of the twenty-four uniform-angle diagrid patterns, for the building with 36, 48, 60, and 72 floors. (For interpretation of the references to colour in this figure legend, the reader is referred to the Web version of this article.)

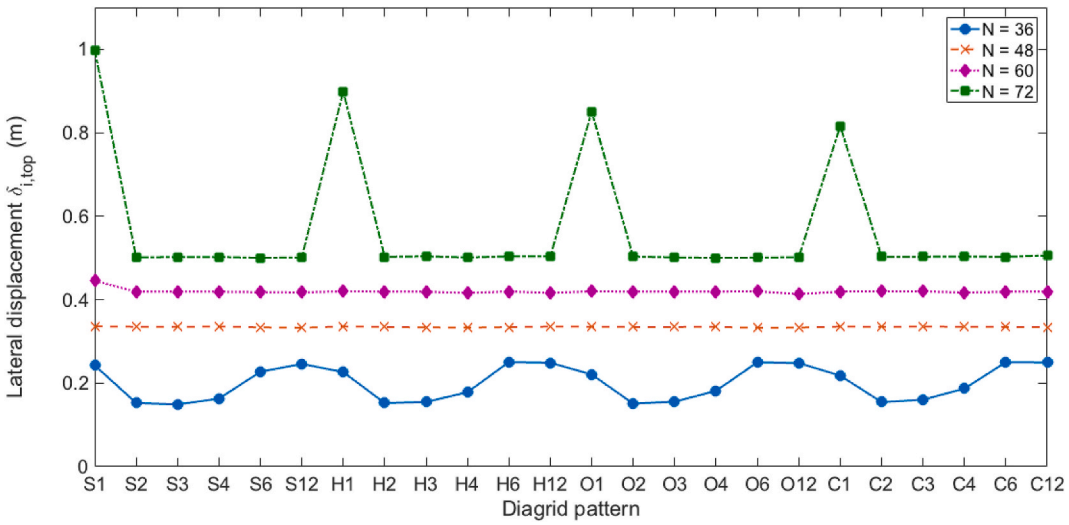

Fig. 5. Lateral displacement at the top of the building $\delta_{i,top}$ (in m) for the twenty-four uniform-angle diagrid patterns, for the building with 36 (continuous blue line), 48 (dashed orange line), 60 (dotted purple line), and 72 (dashed-dotted green line) floors. δ_{lim} (H/500) for the four buildings is equal to 0.25, 0.34, 0.42, and 0.50 m, respectively. (For interpretation of the references to colour in this figure legend, the reader is referred to the Web version of this article.)

The requirements on the maximum displacement also drive the preliminary design of the higher buildings, with $N = 60$ (aspect ratio of 7.0) and $N = 72$ (aspect ratio of 8.4). However, within these populations, some diagrid patterns (S1 for the 60-floor building, and S1, H1, O1, C1, and C12 for the 72-floor building) lead to unfeasible solutions, with $\delta_{i,top} > \delta_{lim}$. This is due to their intrinsic lateral flexibility and, according to case (i) and Equation (7a) reported above, these unfeasible diagrid solutions are assigned values of $d_{i,\delta}$ equal to 0. Conversely, the other patterns in these populations are assigned values of $d_{i,\delta}$ equal to 1, as they are associated to case (ii) and, thus, they follow Equation (7b).

Fig. 6 reports the maximum values of the demand-to-capacity ratio (DCR) for the top and base diagrid modules. From the DCR results, several observations can be made.

First, the DCR values show a recurring trend with respect to the plan floor shape, again confirming that the specific plan shape has only a minor impact on the structure behavior and preliminary design [29]. Figs. S1–S4 in the Supplementary Material show the DCR values of all diagonals, for every square building. The results for the other plan shapes are similar.

Secondly, shorter buildings are mainly designed according to strength, whereas taller buildings are designed according to stiffness [22]. As a matter of fact, the maximum DCR values of the top and base module are very close to 1 for most of the diagrid patterns in the building with $N = 36$. This confirms that, for the preliminary design of this building, strength criteria prevail with respect to stiffness requirements. However, it is interesting to observe that for the diagrid patterns S12, H12, O12, and C12, that correspond to the steepest

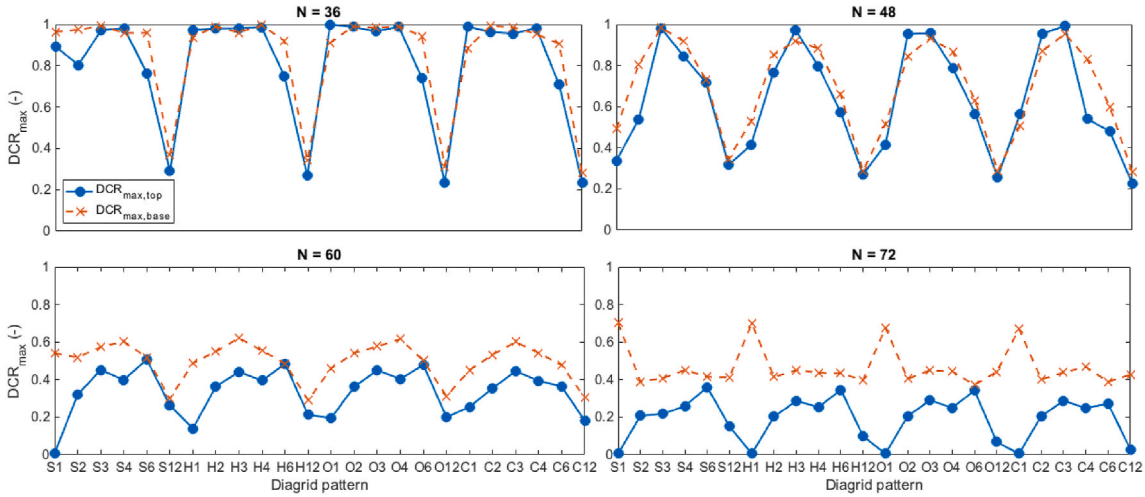

Fig. 6. Maximum demand-to-capacity ratio (DCR) for the top (continuous blue line), and base (dashed orange line) diagrid modules of the twenty-four uniform-angle patterns, for the building with 36, 48, 60, and 72 floors. (For interpretation of the references to colour in this figure legend, the reader is referred to the Web version of this article.)

diagonal inclinations (around 84°), the maximum DCR values are lower than 0.4. This suggests that stiffness requirements prevail with respect to strength constraints for these solutions. In fact, from Fig. 5 we can see that these diagrid patterns are the ones where the top lateral displacement $\delta_{i,top}$ almost reaches the target value δ_{lim}. As already suggested by Mele et al. [24], stiffness vs. strength criteria for the preliminary design of diagrids do not only depend on the building slenderness, but also on the inclination of the diagonals. Very steep diagonals lead to low shear rigidity and, since the lateral deflection of shorter buildings is mainly ruled by shear deformation, this induces the intrinsically large lateral deflection to become the governing parameter for the preliminary design of such solutions.

For the building with $N = 48$ (aspect ratio of 5.6), the maximum DCR values are close to 1 for diagrid patterns with diagonal inclinations in the intermediate range (around 60°–70°). These solutions also reach the target lateral deflection δ_{lim} in the preliminary design, as shown in Fig. 5. This, again, confirms the previous findings from Mele et al. [24], who claimed that an aspect ratio of around 5 can be seen as the threshold between a strength- and a stiffness-based preliminary design. For this building, diagrid patterns with very shallow or very steep diagonals exhibit lower values of maximum DCR. Due to their higher lateral flexibility, their preliminary design turns out to be driven by stiffness rather than by strength requirements.

For the taller buildings, with $N = 60$ (aspect ratio of 7.0) and $N = 72$ (aspect ratio of 8.4), it is evident that the preliminary design is entirely governed by stiffness criteria for all diagrid solutions. The maximum DCR values are generally low (often lower than 0.6), while the top lateral displacement $\delta_{i,top}$ always reaches, and sometimes exceeds, the target limit δ_{lim} (see Fig. 5).

3.1.2. Selection of the optimal geometry based on the desirability function

In this paragraph, the selection of the optimal diagrid geometry within the population of the twenty-four uniform-angle patterns for each building is carried out based on the desirability function approach. Based on the structure properties arising from the preliminary design reported in the previous section, Figs. 7–9 show the additional three responses that are taken into account within the multi-response framework. Fig. 7 reports the values of the torsional rotations at the top of the building under the effect of the eccentric wind action. Fig. 8 displays the total weight of the diagrid system for each pattern, while Fig. 9 reports the values of the complexity index, calculated according to Equation (2). These values are reported for each building and diagonal pattern.

From Fig. 7 it can be observed that the torsional flexibility of the diagrid increases as the number of intra-module floors, $n_{f,m}$, increases, i.e., the torsional flexibility of the building increases as the diagonals become steeper. As firstly shown in [29], this is because the torsional stiffness of the tube only depends on the shear rigidity of the diagrid module. Since steeper diagonals have lower shear rigidity, the torsional flexibility of the building increases for steeper diagonals. According to Equation (4), this results in a higher desirability values $d_{i,\varphi}$ for diagrid patterns with shallower diagonals. Fig. 7 also shows that the specific plan shape has only a minor effect on the torsional rigidity of the diagrid, with a slightly stiffer behavior for rounder shapes. All the values of the torsional rotations for each diagrid pattern and building height are reported in Table S18 in the Supplementary Material. These values show that the most torsionally deformable pattern is S12 for all buildings, with φ_{top} values equal to 21.8, 27.3, 31.3, and 31.4 $\times$ 10^{-4} radians, for the 36-, 48-, 60-, and 72-floor building, respectively. Conversely, the most torsionally rigid patterns for the four buildings are C1, H1, S1, and C1, with φ_{top} values equal to 0.93, 0.85, 0.56, and 0.71 $\times$ 10^{-4} radians, respectively. As can be seen, maximum values of torsional rotations can be up to forty times higher than the minimum values, showing that the diagonal inclination deeply impacts the torsional behavior of the building.

Fig. 8 shows the total amount of steel required for the diagrid system. As can be seen, there exists a range of intermediate diagonal

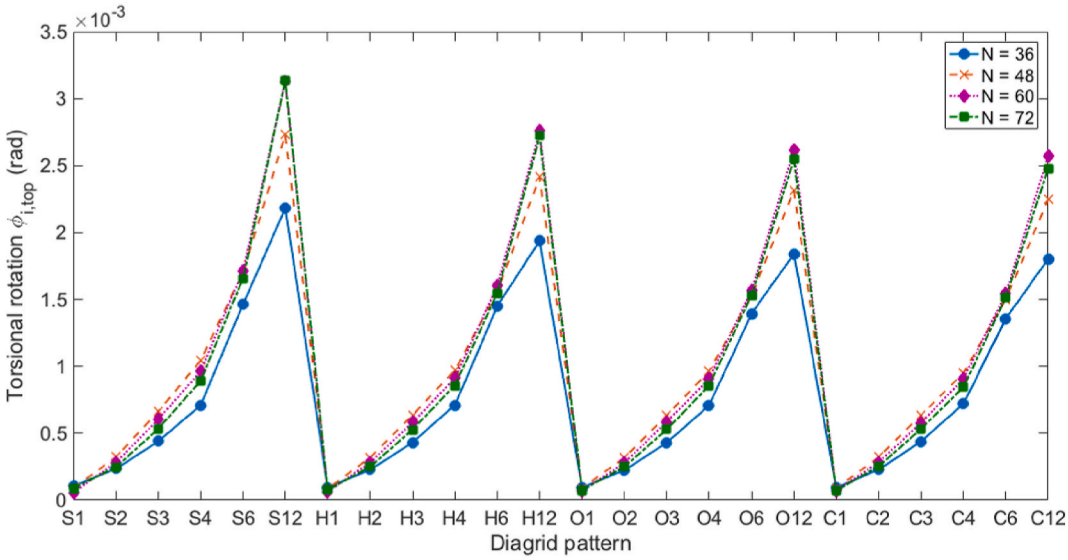

Fig. 7. Torsional rotation at the top of the building $\varphi_{i,top}$ (in rad) for the twenty-four uniform-angle diagrid patterns, for the building with 36 (continuous blue line), 48 (dashed orange line), 60 (dotted purple line), and 72 (dashed-dotted green line) floors. (For interpretation of the references to colour in this figure legend, the reader is referred to the Web version of this article.)

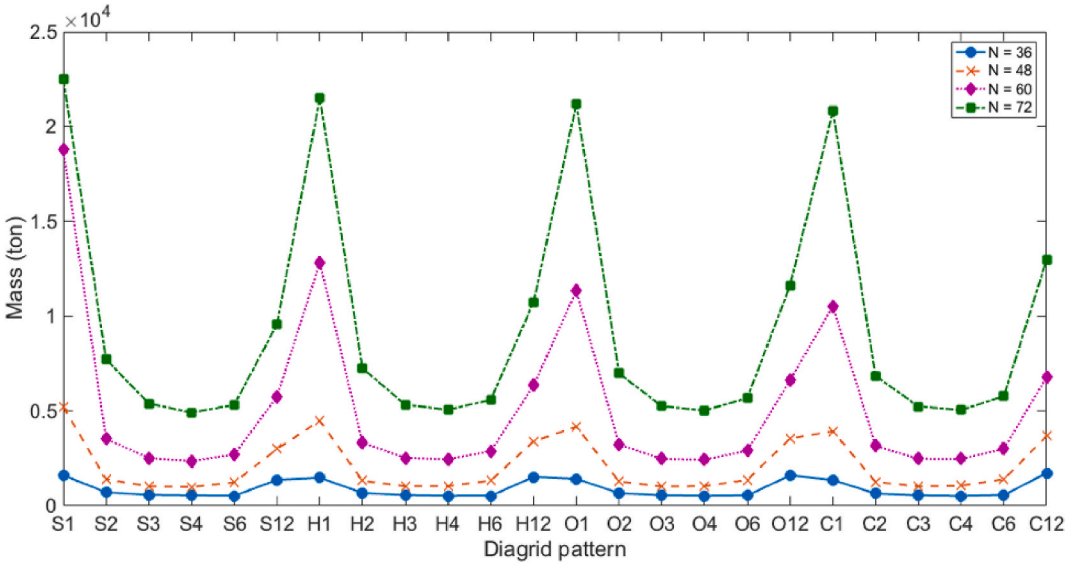

Fig. 8. Diagrid weight W_i (in ton) for the twenty-four uniform-angle diagrid patterns, for the building with 36 (continuous blue line), 48 (dashed orange line), 60 (dotted purple line), and 72 (dashed-dotted green line) floors. (For interpretation of the references to colour in this figure legend, the reader is referred to the Web version of this article.)

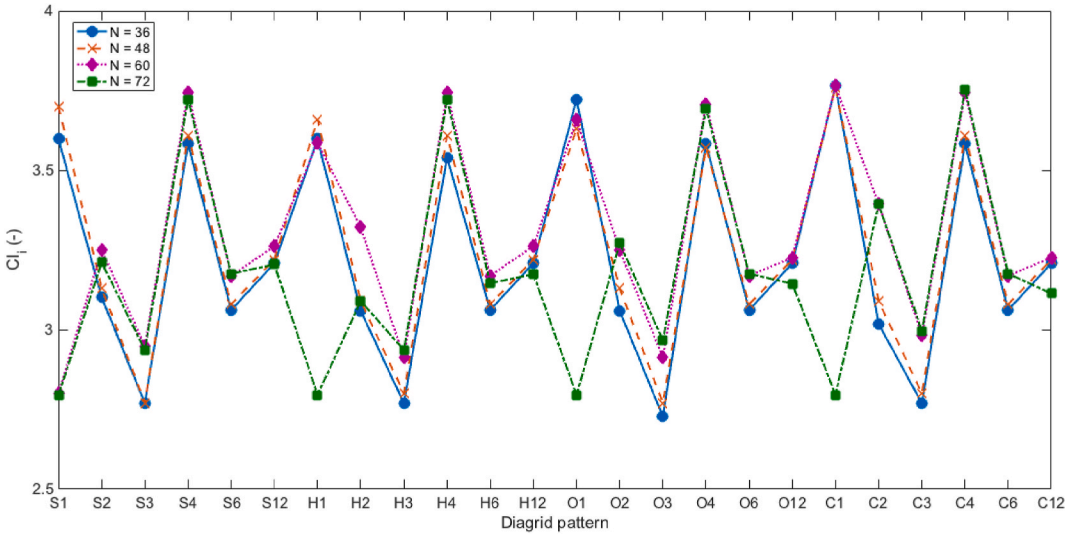

Fig. 9. Complexity index CI_i for the twenty-four uniform-angle patterns, for the building with 36 (continuous blue line), 48 (dashed orange line), 60 (dotted purple line), and 72 (dashed-dotted green line) floors. (For interpretation of the references to colour in this figure legend, the reader is referred to the Web version of this article.)

inclinations where the amount of material is minimum, this range being around 65°–70° ($n_{f,m} = 3$ and 4). Again, the influence of the specific plan shape is marginal, the diagonal inclination playing a more important role. Diagrid patterns with low amount of structural weight result in higher values of the desirability score $d_{i,W}$ according to Equation (5). The complete list of weight values for each diagrid pattern and building height is reported in Table S19 in the Supplementary Material. The heaviest patterns are C12 for the 36-floor building, with a value of W equal to 1726 tons, and S1 for the 48-, 60-, and 72-floor buildings, with W values of 5204, 18780, and 22536 tons, respectively. Conversely, the lightest patterns are C4 for the 36-floor building, with a value of W equal to 510 tons, and S4 for the taller buildings, with W values equal to 991, 2358, and 4916 tons, respectively. The maximum values of diagrid weight can be up to four times higher than the minimum ones, confirming that the diagonal inclination plays a pivotal role in minimizing the structural weight.

The construction complexity index CI_i is reported in Fig. 9. As mentioned above, the range of the CI is between 0 and 5. All solutions are found to have complexity indexes between 2.7 and 3.8. The values of the CI for each diagrid pattern and building height are reported in Tables S20–S23 in the Supplementary Material. The differences among these values depend on the different number of

nodes (N_1) and diagonals (N_4), different number of cross-sections used in the pattern (N_2), and number of slices up to 12 m for transportation issues (N_3). The data reported in Tables S20–S23 show that N_1 increases as the number of intra-module floors $n_{f,m}$ increases, i.e., as the diagonals in the pattern become steeper, whereas N_2 and N_4 decrease. The trend of N_3 is more complex. This is equal to 0 for patterns with diagonals shorter than 12 m, i.e., for diagrids with $n_{f,m}$ up to 3, whereas it reaches maximum values for configurations with $n_{f,m}$ equal to 4 and 12. On the other hand, N_5 is equal to 1 for all solutions, because all diagonals have the same length in all patterns. Note that the difference between the five construction complexity parameters for the different floor plan shapes is only related to the variation of N_2, the other variables being independent of the specific plan shape. As a result, *CI* turns out to be almost independent of the specific floor plan shape. Eventually, patterns with higher *CI* will result in a lower desirability score $d_{i,CI}$ according to Equation (6). Conversely, patterns with lower *CI* values result in a higher desirability from a construction perspective.

Based on the obtained values of the four responses, i.e., lateral displacement (Fig. 5), torsional rotation (Fig. 7), diagrid weight (Fig. 8), and complexity index (Fig. 9), the individual and overall desirability scores have been computed for each diagrid pattern, as explained in Section 2.3. Fig. 10 reports the individual desirability values $d_{i,p}$ for each response p in relation to each diagrid pattern i, for each building. The associated numerical values are reported in Tables S24–S27 in the Supplementary Material. As can be observed, these individual desirability scores reflect the obtained values of the four responses shown in Figs. 5 and 7–9. Remember that, for this calculation, all weighting exponents r_p reported in Equations (4–(7) have been set equal to 1.

Based on the obtained individual desirability scores, Fig. 11 reports the overall desirability, computed according to Equation (8). The numerical values of *OD* are also reported in Tables S24–S27 in the Supplementary Material and are presented in Fig. 11 as three-dimensional plots. In these plots, the vertical axis represents the *OD* value, from 0 to 1, while the two horizontal axes are associated with the plan shape (square, hexagon, octagon, circle) and number of intra-module floors $n_{f,m}$ (1, 2, 3, 4, 6, and 12). For all buildings, the most desirable diagrid solution is found to be associated with 3 intra-module floors ($n_{f,m} = 3$). The octagon (O3) is found to be the most desirable shape for $N = 36$ ($OD_{O3} = 0.64$), $N = 48$ ($OD_{73} = 0.64$), and $N = 60$ ($OD_{O3} = 0.74$), whereas the hexagon (H3) is the one with the highest overall desirability for the 72-floor building ($OD_{H3} = 0.72$). Note that these optimal solutions are slightly different than those found in our previous preliminary work [45]. There, we also found that $n_{f,m} = 3$ provided the most desirable layout, but the circular building (C3) was the most desirable. This difference is mainly related to two reasons. First, vertical loads and stiffness- and strength-based requirements are used here for the preliminary design of the diagrids, therefore the resulting cross-sectional areas are different for each solution; conversely, in [45], we simply assigned all the patterns the same cross-sectional areas and evaluated their performance only under lateral and torque actions. Secondly, here we evaluated the individual desirability values according to Equations (4–(7); conversely, in our previous preliminary work [45], all individual desirability were defined by comparing the values of each response to the minimum and maximum values found within the population (see Equation (2) in Ref. [45]). These two reasons of course lead to a slightly different evaluation of the building performances. The study conducted here is hence a more comprehensive and realistic assessment of the diagrid performance.

As can be easily appreciated by the numerical values of *OD* reported in Tables S24–S27 in the Supplementary Material, the difference between the different plan shapes is only marginal, suggesting once again that the specific plan shape only plays a minor role in defining the efficiency of the diagrid. This is also confirmed by the fact that the *OD* surfaces shown in Fig. 11 are cylindrical in the direction of the plan shape axis. Conversely, the number of intra-module floors, i.e., the diagonal inclination, deeply affects the structural response, and eventually the overall desirability of the diagrid pattern.

Diagrid solutions with three intra-module floors ($n_{f,m} = 3$), corresponding to a diagonal inclination of about 65°, are found to be the most desirable pattern for all buildings. At first sight, this result might seem in contrast with previous findings, where the optimal

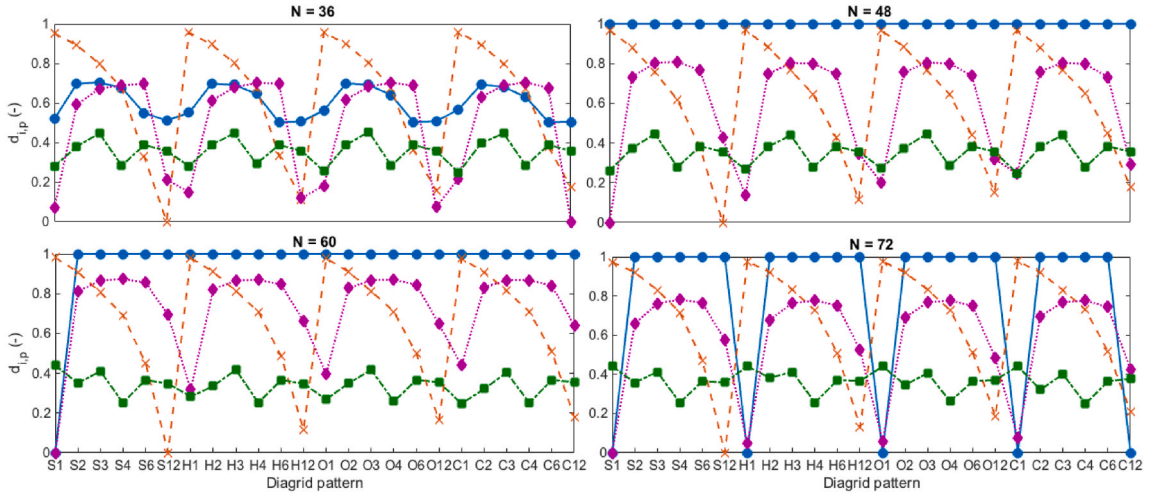

Fig. 10. Individual desirability values $d_{i,p}$ for each diagrid pattern i in relation to each of the four responses p, i.e., $\delta_{i,top}$ (continuous blue line with circle markers), $\varphi_{i,top}$ (dashed orange line with cross markers), W_i (dotted purple line with diamond markers), and CI_i (dashed-dotted green line with square markers), for the building with 36, 48, 60, and 72 floors. (For interpretation of the references to colour in this figure legend, the reader is referred to the Web version of this article.)

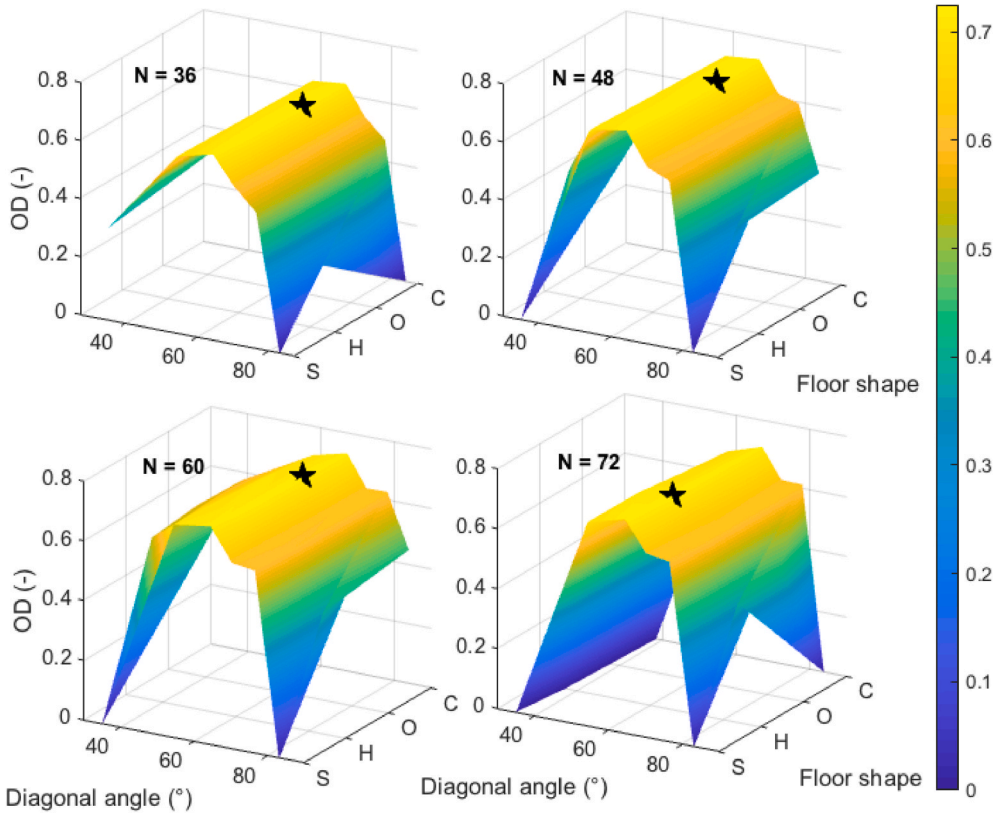

Fig. 11. Overall desirability values OD_i for each diagrid pattern i, for the building with 36, 48, 60, and 72 floors. The *OD* values are reported here as an interpolated surface in the 3D space. The vertical axis represents the value of the *OD*, while the horizontal axes are associated with the two geometrical features of each diagrid pattern, i.e., plan shape and number of intra-module floors $n_{f,m}$. Colors are drawn according to the *OD* values ranging from dark blue (minimum *OD*) to bright yellow (maximum *OD*). Black stars identify the solutions with the highest overall desirability (O3 for $N = 36$, O3 for $N = 48$, O3 for $N = 60$, and H3 for $N = 72$). (For interpretation of the references to colour in this figure legend, the reader is referred to the Web version of this article.)

diagonal inclination was found to increase as the building becomes taller [19,22–24,26,29,32–35]. However, this is not actually surprising here. In the previous works, the optimal diagonal arrangement was selected as the one leading to the minimum diagrid weight, while complying with lateral displacements and strength requirements. The torsional flexibility of the structure, as well as the construction complexity, did not play any role in the definition of the optimal pattern. In this analysis, these two additional responses have been explicitly considered for the selection of the optimal pattern. As a result, the performance of the diagrid solution is not only evaluated in terms of structural mass and lateral displacements, but also in terms of torsional rigidity and construction complexity.

If only the diagrid weight and lateral displacements are considered, steeper diagonals would certainly be more suitable for taller buildings. However, we have seen that steeper diagonals are detrimental for the limitation of torsional rotations (see Fig. 7). Moreover, the diagrid patter with four intra-module floors ($n_{f,m} = 4$), which corresponds to a diagonal inclination of about 70°, is performing worse than the one with three intra-module floors from a construction perspective (see Fig. 9). This is mainly because the 70° solution has diagonals longer than 12 m, which pose more transportation issues. This is explicitly considered in the parameter N_3 for the calculation of the *CI*. As a result, if the torsional flexibility and construction complexity of the diagrid are also taken explicitly into account within the calculations, it is then not surprising that the most desirable diagrid pattern remains the one with three intra-module floors (65°), rather than the one with four (70°), even if the height of the building increases.

As a final remark, from Fig. 11 and Tables S24–27 it can be noted that the diagrid patterns with two intra-module floors (with diagonal inclinations of about 55°), i.e., S2, H2, O2, and C2, exhibit similar, although slightly lower, values of *OD* than the better-performing ones. As a matter of fact, the *OD* values for diagrid patterns with two intra-module floors differ from the maximum ones of only 0.01–0.03. This suggests that for the investigated buildings, both patterns with two and three intra-module floors are the most desirable. The former exhibit a better performance in terms of torsional flexibility (Fig. 7), while the latter are more desirable in relation to the structural weight (Fig. 8) and construction complexity (Fig. 9). From the competition between the different response-based individual performances, the patterns with three intra-module floors turn out to be the most desirable.

3.2. Varying-angle diagrids

In the previous section, the MBM and desirability function approach have been applied for the selection of the optimal geometry within a small population of twenty-four uniform-angle diagrid patterns per building. In this section, the same approach is applied to a

wider population of diagrid geometries with varying-angle patterns. According to the geometrical definition of these patterns laid out in Section 2.2.2, a total of 9728, 31040, 79432, and 175008 diagrid patterns is considered for the 36-, 48-, 60-, and 70-floor building, respectively.

3.2.1. *Preliminary member sizing*

Fig. 12 shows the maximum and minimum cross-sectional areas for the base and top diagonal modules, respectively, upon member sizing. The diagrid patterns are numbered so that the first quarter corresponds to square diagrids, the second quarter to hexagons, the third quarter to octagons, and the last quarter to circular buildings (see upper panels in Fig. 12).

As can be seen from the graphs, the values of cross-sectional areas show a similar trend with respect to the different plan floor shapes. This suggests once again that the specific plan geometry plays a somewhat minor role in the preliminary member sizing. Conversely, within the same plan-shape population, the diagonal pattern has a stronger influence on the required cross-sectional area. Although most of the solutions show similar values of maximum and minimum cross-sectional areas, the distribution across the height of the building changes significantly. As depicted in Fig. 12, some diagrid patterns exhibit high peaks in the cross-sectional area values, suggesting that these geometries are not efficient since they require high amount of material to satisfy the stiffness and strength criteria. Not surprisingly, these diagrid solutions are found to be associated to patterns with very shallow diagonals spread all over the height of the building. These solutions were already found as the ones requiring the most massive cross-sections due to their huge lateral deformability within the uniform-angle population (see Fig. 4).

Fig. 13 reports the obtained lateral displacements under wind load for each diagrid pattern and for each building. As already reported for the uniform-angle population (see Fig. 5), these results show that: (i) for the shortest building ($N = 36$, aspect ratio of 4.2), the strength conditions mainly rule the preliminary design for most of the diagrid solutions, since in most cases the obtained lateral displacement is lower than the limit design value ($\delta_{i,top} < \delta_{lim} = 0.25$ m), with values of $\delta_{i,top}$ as low as 0.15 m; (ii) for the building with $N = 48$ (aspect ratio of 5.6), the stiffness requirement plays a major role, since all the diagrid solutions are now reaching (or approaching very closely) the limit value $\delta_{lim} = 0.336$ m; (iii) for the tallest buildings ($N = 60$, aspect ratio of 7.0, and $N = 72$, aspect ratio of 8.4), the stiffness requirements govern the preliminary design, since the target displacement values δ_{lim} (0.42 m and 0.50 m, respectively) are met. It needs to be noted that, as already observed in Fig. 5 for the uniform-angle population, in the case of $N = 60$ and $N = 72$, there are some diagrid solutions that exceed the limit value δ_{lim} (see the spikes in the lower panels of Fig. 13). These correspond to patterns with very shallow diagonals, which are so inherently flexible under lateral loads that no CHS diagonals are large enough to satisfy the stiffness demand of the structure. In turn, these patterns were the same leading to the maximum values of the cross-sectional areas, as shown by the spikes in the lower panels of Fig. 12. Similar to what discussed above regarding uniform-angle diagrids, these patterns are assigned a value of $d_{i,\delta}$ equal to 0, applying Equation (7a), since they provide an unsatisfactory behavior regarding the lateral flexibility.

Fig. 14 shows the maximum values of the DCR for the top and base diagrid modules, for all varying-angle diagrid patterns and for each building. The DCR results clarify once again that, as the building gets taller, the stiffness criteria become more important for the preliminary design. As a matter of fact, in the building with $N = 36$, DCR values very close to 1 are regularly found for both the top and base module for most diagrid patterns. Conversely, for taller buildings, lower DCR values are found, since the condition on the limitation of the lateral displacement ($\delta_{i,top} < \delta_{lim}$) becomes the most severe (see Fig. 13). In these cases, maximum DCR values of 0.6–0.9, 0.4–0.6, and 0.2–0.5 are found for the buildings with $N = 48$, 60, and 72, respectively.

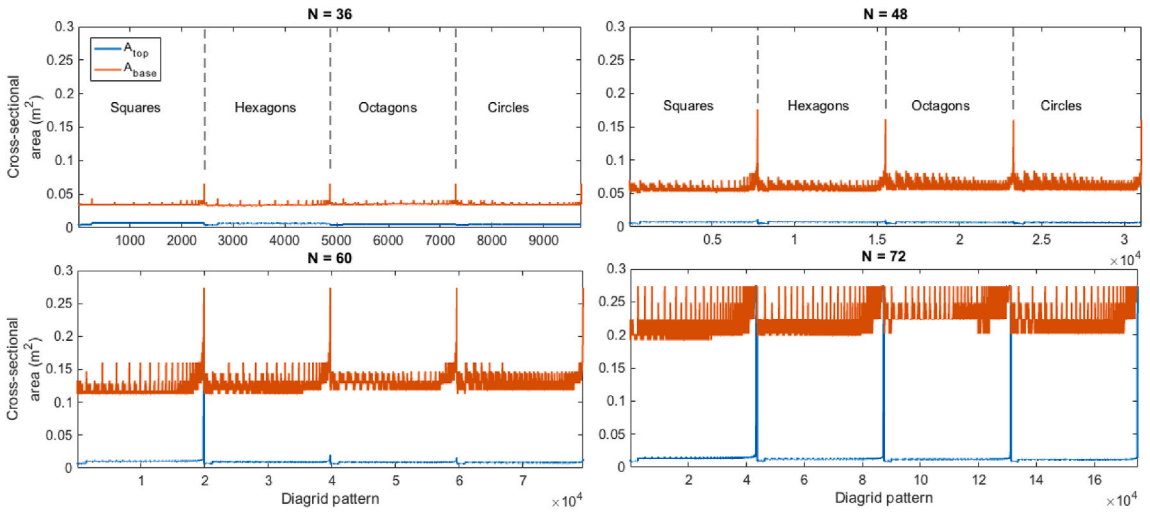

Fig. 12. Cross-sectional areas (in m^2) for the top (blue line) and base (orange line) modules of all varying-angle diagrid patterns, for the building with 36, 48, 60, and 72 floors. Diagrid pattern numbers are defined according to the specific combination of different diagrid modules with different diagonal combinations. As a general trend, higher diagrid pattern numbers are associated to the presence of diagrid modules with shallower diagonals (see Fig. 3). The first quarter of the pattern numbers refer to the square diagrids, the second quarter to the hexagons, the third quarter to the octagons, and the last quarter to the circles. (For interpretation of the references to colour in this figure legend, the reader is referred to the Web version of this article.)

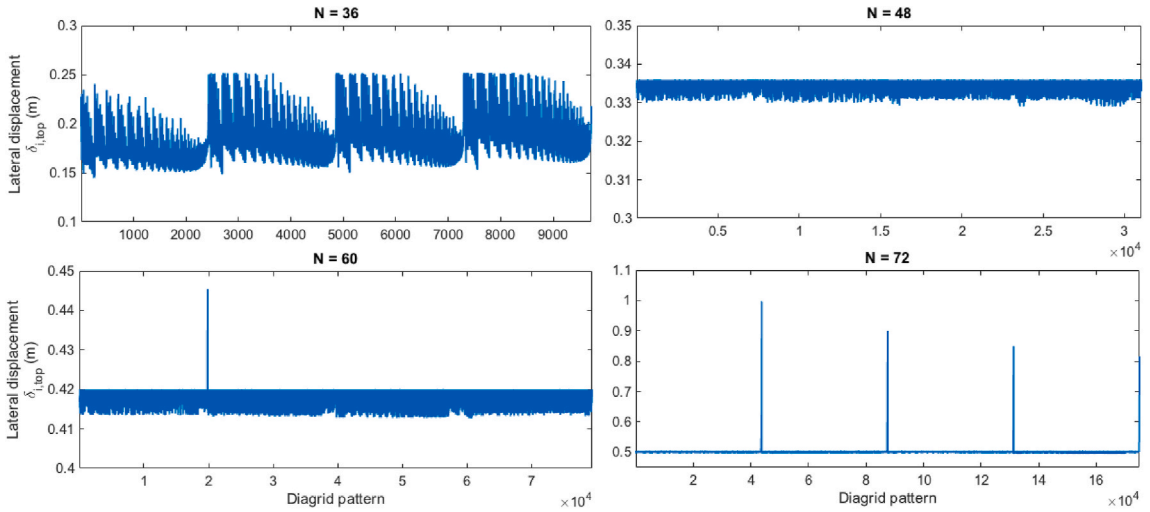

Fig. 13. Lateral displacement at the top of the building $\delta_{i,top}$ (in m) for all varying-angle diagrid patterns, for the building with 36, 48, 60, and 72 floors. δ_{lim} (H/500) for the four buildings is equal to 0.25, 0.34, 0.42, and 0.50 m, respectively.

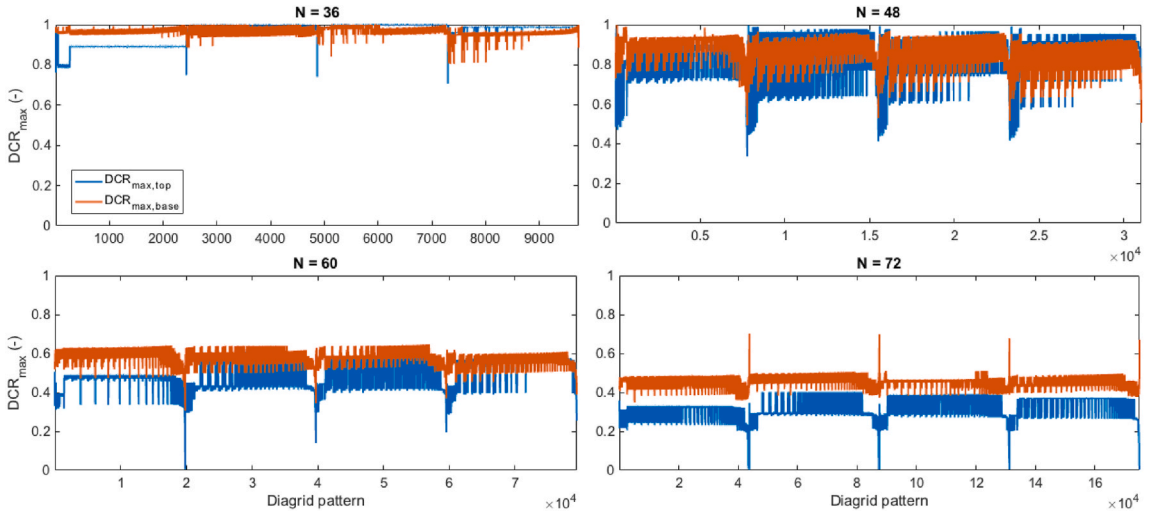

Fig. 14. Maximum demand-to-capacity ratio (DCR) for the top (blue line) and base (orange line) diagrid modules of all varying-angle diagrid patterns, for the building with 36, 48, 60, and 72 floors. (For interpretation of the references to colour in this figure legend, the reader is referred to the Web version of this article.)

3.2.2. Selection of the optimal geometry based on the desirability function

Based on the structural and geometrical properties of the generated varying-angle diagrid patterns, Figs. 15–17 report the values of the additional responses that are considered within the multi-response framework. Specifically, Fig. 15 shows the values of the torsional rotations, Fig. 16 the total weight of the diagrid, and Fig. 17 the complexity index of each pattern. In relation to Figs. 12–17, note that diagrid patterns have been numbered based on the combination of diagrid modules, in such a way that patterns containing steeper diagonals come before those containing more modules with shallower diagonals (see Fig. 3).

Like what we found for the uniform-angle population, Fig. 15 suggests that torsional rotations generally decrease when modules with shallower diagonals are included into the pattern. The maximum torsional rotation obtained in the 36-floor building population is 15.33×10^{-4} radians, which is associated to the pattern #261 and corresponds to the square building with $M_1 = 1, M_2 = M_3 = M_4 = 0$, $M_5 = 1$, and $M_6 = 5$. On the other hand, the minimum torsional rotation obtained within this population is equal to 0.93×10^{-4} radians, and corresponds to the pattern #9728, which is the circular building with $M_1 = 36$, and $M_2 = M_3 = M_4 = M_5 = M_6 = 0$ (this solution basically represents the uniform-angle pattern C1). For the 48-floor building, the maximum and minimum torsional rotations are 17.02 and 0.85×10^{-4} radians, respectively, which are associated to patterns #1 and #15520. The former corresponds to the square building with $M_1 = M_2 = M_3 = M_4 = M_5 = 0$, and $M_6 = 8$ (which represents the uniform-angle pattern S6), while the latter corresponds to the hexagonal building with $M_1 = 48$, and $M_2 = M_3 = M_4 = M_5 = M_6 = 0$ (which represents the uniform-angle pattern H1). For the 60-floor building, the maximum and minimum values of the rotation are 17.27 and 0.56×10^{-4} radians, which are

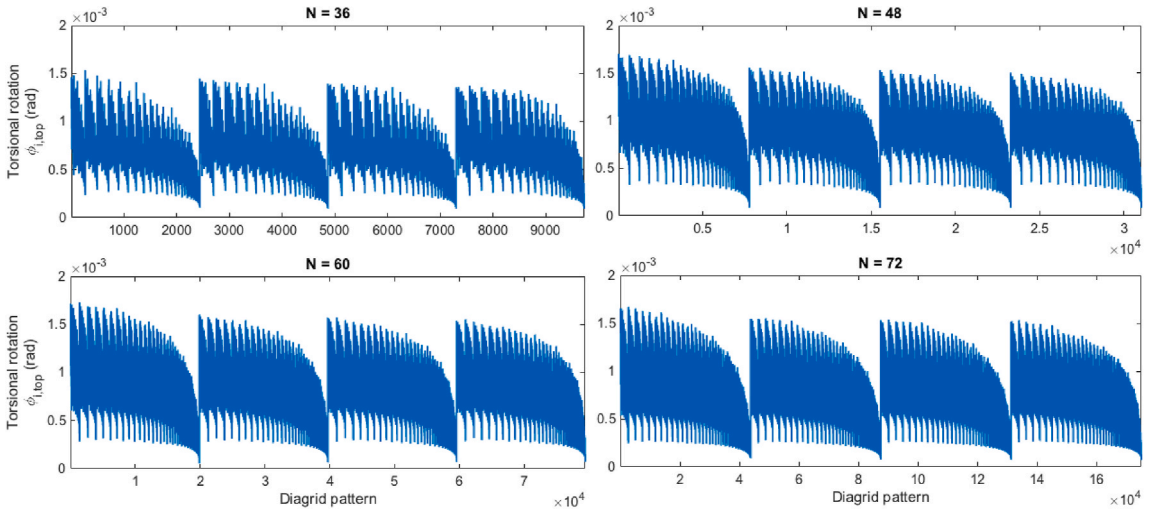

Fig. 15. Torsional rotation at the top of the building $\varphi_{i,top}$ (in rad) for all varying-angle diagrid patterns, for the building with 36, 48, 60, and 72 floors.

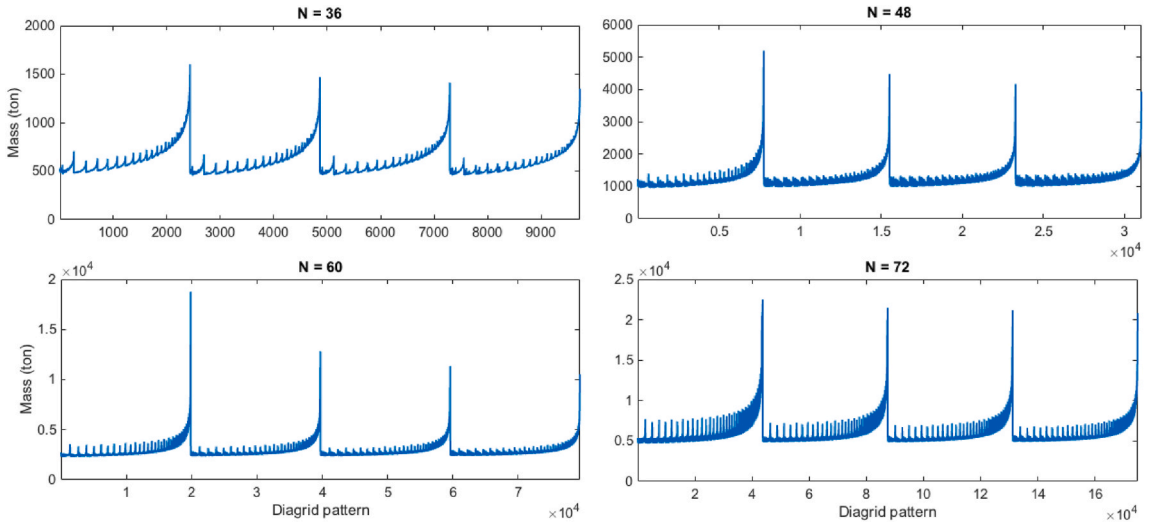

Fig. 16. Diagrid weight W_i (in ton) for all varying-angle diagrid patterns, for the building with 36, 48, 60, and 72 floors.

associated to patterns #1392 and #19858, respectively. The former corresponds to the square building with $M_1 = 1$, $M_2 = M_3 = M_4 = 0$, $M_5 = 1$, and $M_6 = 9$, while the latter corresponds to the square building with $M_1 = 60$, and $M_2 = M_3 = M_4 = M_5 = M_6 = 0$ (which represents the uniform-angle pattern S1). Finally, in the 72-floor building, the maximum and minimum rotations are 16.73 and 0.71×10^{-4} radians, respectively, which are associated to patterns #2619 and #175008. The former corresponds to the square building with $M_1 = 1$, $M_2 = M_3 = M_4 = 0$, $M_5 = 1$, and $M_6 = 11$, while the latter corresponds to the circular building with $M_1 = 72$, and $M_2 = M_3 = M_4 = M_5 = M_6 = 0$ (which represents the uniform-angle pattern C1). According to Equation (4), the patterns corresponding to the maximum values of $\varphi_{i,top}$ are assigned a desirability value $d_{i,\varphi}$ equal to 0, while all other patterns will have higher values of individual desirability values. The lower the value of their associated torsional rotation, the higher their individual desirability $d_{i,\varphi}$.

Fig. 16 shows that the mass of the diagrid generally increases significantly for patterns including more modules with shallower diagonals. The maximum diagrid weight obtained within the 36-floor building population is found to be 1603 tons, which is associated to the pattern #2432 and corresponds to the square building with $M_1 = 36$, and $M_2 = M_3 = M_4 = M_5 = M_6 = 0$ (which basically represents the uniform-angle pattern S1). On the other hand, the minimum value of diagrid weight obtained within this population is equal to 454 tons, and corresponds to the pattern #2484, which is the hexagonal building with $M_1 = 0$, $M_2 = 1$, $M_3 = 0$, $M_4 = 7$, $M_5 = 0$, and $M_6 = 1$. For the 48-floor building, the maximum and minimum values of diagrid weight are 5204 and 946 tons, respectively, which are associated to patterns #7760 and #970. The former corresponds to the square building with $M_1 = 48$, and $M_2 = M_3 = M_4 = M_5 = M_6 = 0$ (which represents the uniform-angle pattern S1), while the latter corresponds to the square building with $M_1 = 1$, $M_2 = 4$, $M_3 = 6$, $M_4 = 4$, $M_5 = 1$, and $M_6 = 0$. For the 60-floor building, the maximum and minimum values of the diagrid weight are 18780 and 2257

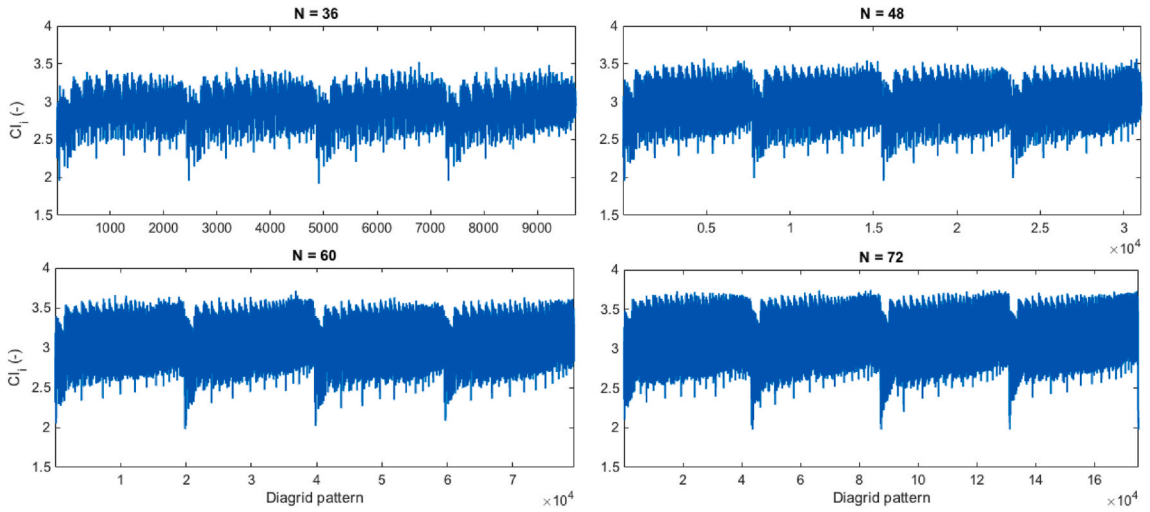

Fig. 17. Complexity index CI_i for all varying-angle diagrid patterns, for the building with 36, 48, 60, and 72 floors.

tons, which are associated to patterns #19858 and #1869, respectively. The former corresponds to the square building with $M_1 = 60$, and $M_2 = M_3 = M_4 = M_5 = M_6 = 0$ (which represents the uniform-angle pattern S1), while the latter corresponds to the square building with $M_1 = 1$, $M_2 = 3$, $M_3 = 7$, $M_4 = 4$, $M_5 = 2$, and $M_6 = 1$. Finally, in the 72-floor building, the maximum and minimum values of diagrid weight are found to be equal to 22536 and 4687 tons, respectively, which are associated to patterns #43752 and #603. The former corresponds to the square building with $M_1 = 72$, and $M_2 = M_3 = M_4 = M_5 = M_6 = 0$ (which represents the uniform-angle pattern S1), while the latter corresponds to the square building with $M_1 = 32$, $M_2 = 1$, $M_3 = 1$, $M_4 = 6$, $M_5 = 1$, and $M_6 = 1$. According to Equation (5), the patterns corresponding to the maximum values of W_i are assigned a desirability value $d_{i,W}$ equal to 0, while all other patterns have higher values of individual desirability values. The lower the value of their associated structural weight, the higher their individual desirability $d_{i,W}$.

Fig. 17 shows that the complexity index exhibits no obvious trends within the population. All patterns have complexity indexes in the range 2.0–3.5. The specific value of *CI* depends on the values of the five geometry-dependent parameters N_1, N_2, N_3, N_4, N_5. The variation of these five parameters for all diagrid patterns is reported in the Supplementary Material in Figs. S5–S9.

Fig. S5 reports the value of N_1, i.e., the weighted number of nodes, for each diagrid pattern and for each building. As can be seen from this figure, diagrid patterns with shallower diagonals usually imply a lower number of weighted nodes. As a matter of fact, despite solutions with steeper diagonals usually exhibit a lower number of nodes at the level of diagonal-diagonal connections, they have a higher number of intersections between the diagonals and the numerous intra-module floors. Fig. S6 reports the variation of N_2, i.e., the total number of different cross-sections used in the pattern. This value is generally found to increase for diagrid patterns with shallower diagonals. This is because, due to the lower inclination of the diagonals, these patterns have a higher number of diagrid modules, hence generally a higher number of different cross-sections. Fig. S7 shows the trend of N_3, which represents the number of splices required for diagonals longer than 12 m, which are needed for transportation. Obviously, this value increases for diagrid patterns including longer diagonals, i.e., those with steeper diagonals. Fig. S8 reports the values of N_4, i.e., the total number of diagonals in the pattern, which increases as the diagonals become shallower. Finally, Fig. S9 shows the trend of N_5, which represents the number of different diagonal lengths in the pattern. This value can be an integer number between a minimum value of 1, which corresponds to uniform-angle geometries where all diagonals have the same length, and a maximum value of 6, which corresponds to patterns which include all six different diagrid modules. As can be seen from Fig. S9, N_5 has no clear trend as a function of diagonal inclination since it strongly depends on the specific combination of different diagrid modules.

Based on the obtained values of the four responses, i.e., lateral displacement (Fig. 13), torsional rotation (Fig. 15), diagrid weight (Fig. 16) and complexity index (Fig. 17), the individual and overall desirability scores have been computed for each diagrid pattern. Figs. S10–S13 in the Supplementary Material report the individual desirability values $d_{i,p}$ for each response p in relation to each diagrid pattern i and for each building. These individual desirability scores reflect the obtained values of the four responses shown in Figs. 13 and 15–17. Again, all weighting exponents r_p have been set equal to 1 here for the four responses.

Based on the individual desirability values reported in Figs. S10–S13, Equation (8) yields the calculation of the *OD* scores, which are reported in Fig. 18. The analysis of *OD* values across the population leads to the selection of the most desirable diagrid patterns. Fig. 19 shows the distribution of *OD* values across the diagrid populations for the four buildings. The most desirable pattern, i.e., the one with maximum *OD*, is highlighted in Figs. 18 and 19 with a black star. Note from Fig. 19 that *OD* values typically distribute as a normal variable: most of the patterns exhibit *OD* scores around the average value, while only a relatively small number of individuals within the population exhibits very small or very high values of *OD*. The detailed features of the fifteen most desirable diagrid geometries, i.e., the fifteen with the highest *OD* scores, are reported in Tables 2–5 for the 36-, 48-, 60-, and 72-floor building, respectively.

For the 36-floor building, diagrid pattern #4908 was found to be the most desirable, with a maximum *OD* value of 0.67. This pattern corresponds to the octagonal uniform-angle pattern with twelve modules, each made up of three intra-module floors, i.e., O3.

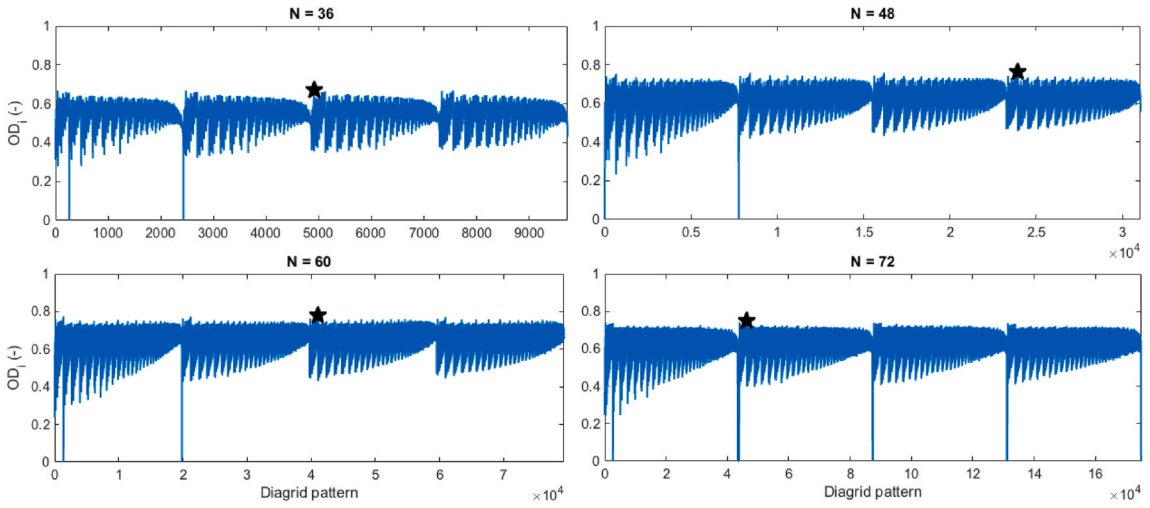

Fig. 18. Overall desirability values OD_i for each diagrid pattern i, for the building with 36, 48, 60 and 72 floors. Black stars identify the solutions with the highest overall desirability, i.e., pattern #4908 for the 36-floor building, pattern #23936 for the 48-floor building, pattern #41107 for the 60-floor building, and pattern #46370 for the 72-floor building.

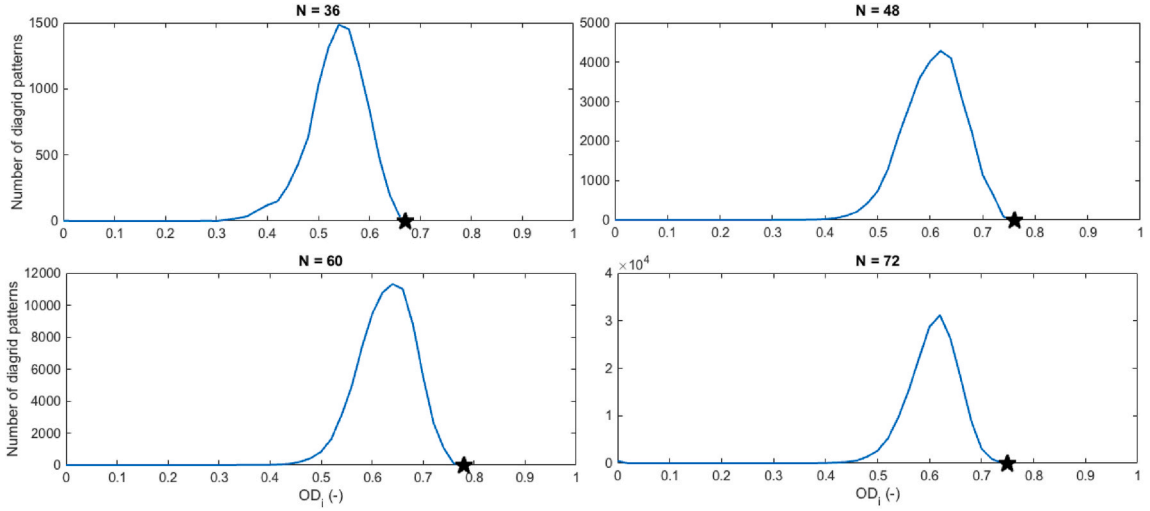

Fig. 19. Distribution of overall desirability values OD_i, for the building with 36, 48, 60 and 72 floors. Black stars identify the solutions with the highest overall desirability, i.e., pattern #4908 for the 36-floor building, pattern #23936 for the 48-floor building, pattern #41107 for the 60-floor building, and pattern #46370 for the 72-floor building.

Table 2 also shows the individual desirability scores of this pattern with respect to each response, i.e., $d_{4908,\delta}$ (0.69), $d_{4908,\varphi}$ (0.72), $d_{4908,W}$ (0.66), and $d_{4908,CI}$ (0.62). As can be observed, the overall good performance of this pattern comes from good individual performances for each response. Table 2 also shows that there are other diagrid geometries with similar values of OD (the fifteen most desirable patterns have OD values clustered in the range 0.66–0.67). Notably, many of them (7 out of the 15 reported in Table 2) are uniform-angle geometries, e.g., H3 (second best score, with $OD = 0.667$), C2 (third best score, with $OD = 0.667$), S3 (fourth best score, with $OD = 0.667$), etc. The other 8 geometries correspond to actual varying-angle patterns. Notably, these varying-angle geometries arise always from a mixture of modules made of two or three intra-module floors, i.e., $M_1 = M_4 = M_5 = M_6 = 0$, while $M_2 \neq 0$ and $M_3 \neq 0$. The individual desirability values of these diagrid patterns are similar to each other. However, some differences arise, which in turn affect the final value of OD and thus the overall performance of each pattern. For example, diagrid pattern #5124, which corresponds to the octagonal uniform-angle geometry with two intra-module floors (O2), ends up being the eighth most desirable overall, with an OD of 0.663, although it is the best performing in this group as regards the torsional rotation ($d_{5124,\varphi} = 0.853$). The lower performances of this pattern in terms of structural mass ($d_{5124,W} = 0.558$) and construction complexity ($d_{5124,CI} = 0.551$) make this pattern not the most desirable overall.

Tables 3–5 show the same results reported in Table 2, but for the taller buildings, i.e., for the building with 48, 60, and 72 floors, respectively. The most desirable pattern for the 48-floor building turns out to be the circular uniform-angle diagrid with two intra-

Table 2
The fifteen most desirable diagrid patterns for the 36-floor building, ordered for decreasing value of *OD*.

#	Diagrid patter no.	Floor shape	M_1	M_2	M_3	M_4	M_5	M_6	$d_{i,\delta}$	$d_{i,\varphi}$	$d_{i,W}$	$d_{i,CI}$	*OD*
1	4908 (O3)	O	0	0	12	0	0	0	0.691	0.719	0.658	0.617	0.670
2	2476 (H3)	H	0	0	12	0	0	0	0.692	0.718	0.655	0.609	0.667
3	7556 (C2)	C	0	18	0	0	0	0	0.693	0.851	0.601	0.559	0.667
4	44 (S3)	S	0	0	12	0	0	0	0.704	0.713	0.647	0.609	0.667
5	7340 (C3)	C	0	0	12	0	0	0	0.682	0.713	0.665	0.609	0.666
6	7554	C	0	15	2	0	0	0	0.696	0.823	0.621	0.547	0.664
7	7547	C	0	12	4	0	0	0	0.692	0.793	0.641	0.551	0.664
8	5124 (O2)	O	0	18	0	0	0	0	0.700	0.853	0.588	0.551	0.663
9	5115	O	0	12	4	0	0	0	0.701	0.798	0.633	0.542	0.662
10	7530	C	0	9	6	0	0	0	0.685	0.764	0.657	0.555	0.661
11	2666	H	0	9	6	0	0	0	0.693	0.766	0.647	0.555	0.661
12	200	S	0	6	8	0	0	0	0.696	0.732	0.650	0.576	0.661
13	2692 (H2)	H	0	18	0	0	0	0	0.698	0.851	0.580	0.551	0.660
14	5098	O	0	9	6	0	0	0	0.696	0.769	0.649	0.546	0.660
15	2683	H	0	12	4	0	0	0	0.699	0.795	0.630	0.542	0.660

Table 3
The fifteen most desirable diagrid patterns for the 48-floor building, ordered for decreasing value of *OD*.

#	Diagrid patter no.	Floor shape	M_1	M_2	M_3	M_4	M_5	M_6	$d_{i,\delta}$	$d_{i,\varphi}$	$d_{i,W}$	$d_{i,CI}$	*OD*
1	23936 (C2)	C	0	24	0	0	0	0	1.000	0.810	0.760	0.544	0.761
2	8416 (H2)	H	0	24	0	0	0	0	1.000	0.812	0.748	0.544	0.758
3	16176 (O2)	O	0	24	0	0	0	0	1.000	0.812	0.756	0.537	0.758
4	23934	C	0	21	2	0	0	0	1.000	0.782	0.776	0.534	0.754
5	16174	O	0	21	2	0	0	0	1.000	0.781	0.774	0.534	0.754
6	654	S	0	21	2	0	0	0	1.000	0.777	0.756	0.547	0.753
7	8414	H	0	21	2	0	0	0	1.000	0.783	0.766	0.534	0.752
8	656 (S2)	S	0	24	0	0	0	0	1.000	0.810	0.733	0.537	0.751
9	23927	C	0	18	4	0	0	0	1.000	0.753	0.788	0.530	0.749
10	16150	O	0	15	6	0	0	0	1.000	0.726	0.795	0.540	0.747
11	630	S	0	15	6	0	0	0	1.000	0.716	0.785	0.553	0.747
12	16167	O	0	18	4	0	0	0	1.000	0.755	0.786	0.524	0.747
13	8390	H	0	15	6	0	0	0	1.000	0.728	0.790	0.540	0.747
14	9578	H	2	23	0	0	0	0	1.000	0.805	0.750	0.514	0.746
15	23910	C	0	15	6	0	0	0	1.000	0.726	0.796	0.533	0.745

Table 4
The fifteen most desirable diagrid patterns for the 60-floor building, ordered for decreasing value of *OD*.

#	Diagrid patter no.	Floor shape	M_1	M_2	M_3	M_4	M_5	M_6	$d_{i,\delta}$	$d_{i,\varphi}$	$d_{i,W}$	$d_{i,CI}$	*OD*
1	41107 (O2)	O	0	30	0	0	0	0	1.000	0.837	0.829	0.534	0.780
2	1391 (S2)	S	0	30	0	0	0	0	1.000	0.836	0.812	0.534	0.776
3	21249 (H2)	H	0	30	0	0	0	0	1.000	0.837	0.823	0.522	0.774
4	60965 (C2)	C	0	30	0	0	0	0	1.000	0.835	0.832	0.509	0.771
5	41098	O	0	24	4	0	0	0	1.000	0.800	0.848	0.518	0.770
6	21189	H	0	18	8	0	0	0	1.000	0.757	0.858	0.536	0.768
7	41047	O	0	18	8	0	0	0	1.000	0.758	0.861	0.529	0.767
8	21240	H	0	24	4	0	0	0	1.000	0.800	0.843	0.512	0.767
9	41105	O	0	27	2	0	0	0	1.000	0.816	0.840	0.503	0.767
10	21247	H	0	27	2	0	0	0	1.000	0.817	0.835	0.503	0.766
11	1389	S	0	27	2	0	0	0	1.000	0.813	0.827	0.509	0.765
12	20013 (H3)	H	0	0	20	0	0	0	1.000	0.663	0.866	0.596	0.765
13	39871 (O3)	O	0	0	20	0	0	0	1.000	0.660	0.869	0.596	0.765
14	60963	C	0	27	2	0	0	0	1.000	0.814	0.843	0.497	0.764
15	21223	H	0	21	6	0	0	0	1.000	0.778	0.852	0.514	0.764

module floors, i.e., C2 ($OD = 0.76$). The most desirable one for the 60-floor building is the octagonal uniform-angle diagrid with two intra-module floors, i.e., O2 ($OD = 0.78$). The most desirable for the 72-floor building is the hexagonal uniform-angle diagrid with two intra-module floors, i.e., H2 ($OD = 0.75$). As can be appreciated, despite considering a huge variety of actual varying-angle geometries, uniform-angle diagrids (which represent a particular subset of these populations) are always found to be overall the most desirable patterns. Moreover, as in the case of the 36-floor building, many uniform-angle patterns including two or three floors per module are amongst the list of the fifteen most desirable patterns for all buildings.

At first sight, these results might seem in contrast with some of the previous literature that found that actually-varying-angle

Table 5
The fifteen most desirable diagrid patterns for the 72-floor building, ordered for decreasing value of *OD*.

#	Diagrid patter no.	Floor shape	M_1	M_2	M_3	M_4	M_5	M_6	$d_{i,\delta}$	$d_{i,\varphi}$	$d_{i,W}$	$d_{i,CI}$	*OD*
1	46370 (H2)	H	0	36	0	0	0	0	1.000	0.850	0.678	0.549	0.750
2	46361	H	0	30	4	0	0	0	1.000	0.821	0.713	0.531	0.747
3	46310	H	0	24	8	0	0	0	1.000	0.791	0.738	0.530	0.746
4	46344	H	0	27	6	0	0	0	1.000	0.809	0.725	0.522	0.744
5	46154	H	0	18	12	0	0	0	1.000	0.761	0.752	0.534	0.743
6	46250	H	0	21	10	0	0	0	1.000	0.776	0.747	0.526	0.743
7	44001 (H3)	H	0	0	24	0	0	0	1.000	0.684	0.764	0.579	0.742
8	90122 (O2)	O	0	36	0	0	0	0	1.000	0.849	0.691	0.513	0.741
9	87753 (O3)	O	0	0	24	0	0	0	1.000	0.684	0.767	0.573	0.741
10	249 (S3)	S	0	0	24	0	0	0	1.000	0.681	0.761	0.579	0.740
11	46009	H	0	15	14	0	0	0	1.000	0.745	0.757	0.530	0.739
12	89761	O	0	15	14	0	0	0	1.000	0.742	0.763	0.524	0.738
13	131505 (C3)	C	0	0	24	0	0	0	1.000	0.681	0.768	0.568	0.738
14	2592	S	0	27	6	0	0	0	1.000	0.803	0.716	0.516	0.738
15	90002	O	0	21	10	0	0	0	1.000	0.775	0.753	0.508	0.738

diagrids should be the most performant patterns for taller buildings, due to their higher capability to optimize the bending vs. shear distribution along the building [20,21,32,33]. However, as already mentioned above, in those studies the performance of the diagrid pattern was only assessed in terms of minimum structural weight, while satisfying the required lateral displacement and strength requirements. Here, besides the lateral flexibility and the diagrid weight, the multi-response framework based on the desirability function takes also into account the torsional flexibility and the construction complexity of the pattern. Since these responses are generally worse for varying-angle diagrids compared to uniform-angle geometries, this tends to bias the optimization result towards uniform-angle geometries.

Another interesting outcome of this analysis is that in most of the cases, the most desirable geometries always involve diagrid modules with two or three intra-module floors (see Tables 2–5). Again, this might seem in contrast with the previous literature that showed that as the building becomes taller, we should expect an increase in the optimum diagonal inclination [19,24,32,33,35]. Why, then, don't we obtain optimal diagrid patterns with steeper diagonals for the slenderest buildings? Once again, this is strictly related to the fact that all previous works defined the optimal diagrid pattern as the one minimizing the structural weight, while complying with lateral flexibility criteria. In this case, torsional flexibility and construction complexity responses are also explicitly taken into account for the selection of the optimal geometry. We have already seen in Section 3.1 that shallow diagonals work better for the limitation of the torsional rotations. Moreover, we have seen that diagrid modules with more than three intra-floor modules increase the complexity of the structure due to a higher number of nodes and longer diagonals, which usually require more splices for transportation issues. Putting all this together within the desirability multi-response framework, we obtain the results reported in Tables 2–5, where the optimal diagrid geometry does not follow a precise trend with the increase of the building slenderness, since many responses come now explicitly into play.

4. Conclusions

In this paper, the desirability function approach was applied in combination with the matrix-based method (MBM) to carry out a fast and straightforward optimization analysis, aimed at selecting the optimal diagonal pattern for diagrid tall buildings in a multi-response framework. In particular, the MBM was used to perform the structural analysis and the preliminary sizing of uniform- and varying-angle diagrids under vertical loads and eccentric wind actions. Then, the desirability function was applied to compute the overall desirability (*OD*) of each diagrid pattern, considering the individual desirability scores for four selected responses, i.e., the lateral displacement at the top of the building, the top torsional rotation, the diagrid weight, and the construction complexity. Based on the analysis of the obtained *OD* values, the most desirable diagrid patterns were selected. Differently from the main approaches used in the literature, which used only the minimization of structural weight as the driving optimization parameter, the methodology applied here allowed to consider multiple responses simultaneously to define the optimal diagrid geometry.

From the outcomes, it was observed that, in both uniform- and varying-angle diagrid populations, the specific plan shape of the building plays a minor role, although a slight bias towards more rounded shapes was found. More interestingly, the diagonal angle was found to be the key parameter, affecting the performance of the building dramatically.

4.1. Uniform-angle diagrid population

For the uniform-angle population, diagrid patterns with modules containing three intra-module floors (with diagonal inclination of about 65°) were found to be the most desirable taking simultaneously into account all four responses. Patterns with two intra-module floors (with diagonal inclination of about 55°) were also found quite desirable. Despite the lower performance of patterns with two intra-module floors in terms of structural weight and construction complexity, their torsional behavior was more efficient, hence their *OD* value showed competitive values. Interestingly, it was also found that, as the building becomes taller, the optimal diagonal inclination remains the same. This is not in agreement with previous studies, which found that taller buildings usually require steeper diagonals for optimal performance. However, this comes from the need to minimize not only the lateral displacement of the building and structural weight, but also the torsional flexibility and construction complexity. Although the former responses would require

steeper diagonals for taller buildings, the latter do not. Increasing the diagonal inclination lowers the torsional performance of the diagrid, and steeper diagonals usually lead to higher construction complexity.

4.2. Varying-angle diagrid population

For the wider varying-angle population, it was again found that the floor plan shape plays only a minor role on the building performance. Interestingly, it was found that a particular subset of varying-angle patterns, i.e., uniform-angle geometries, was always found to be amongst the most desirable solutions for all the investigated buildings. In the previous literature, it was found that uniform-angle diagrids are the most efficient for shorter buildings, while actually-varying-angle diagrids should have a prevailing performance for taller buildings. Once again, these outcomes only arise if you consider the optimal geometry as the one only minimizing the structural mass, while complying with strength requirements and the lateral displacement. When you put other responses in the mix, such as the construction complexity and torsional flexibility, the outcomes can change. In this case, the analysis revealed that uniform-angle diagonal patterns are the prevailing optimal layouts for both shorter and taller buildings, because they are more desirable from a torsional and constructional perspective. Again, it was found that diagrid patterns including diagonals spanning over two or three floors (corresponding to diagonal inclinations of about 55°–65°) are the most desirable in this multi-response framework.

4.3. Further considerations

The analysis presented in this paper was based on the adoption of four specific responses, i.e., the lateral and torsional flexibility, the structural weight, and the construction complexity, for the selection of the optimal diagrid pattern. It must be remarked that the same approach could also include other responses that might be of interest to the designer for a particular project. These can include, e.g., the dynamical response of the building under earthquake motions, the energy efficiency of the building, the sustainability of the construction process, the architectural appearance, etc. The optimal diagrid pattern will then be selected accordingly considering the individual performance with respect to these responses. The power of the desirability function approach is that it can include a large variety of responses that are of interest for the designer, which can then be used to drive the optimization process.

Moreover, the method shown in this paper was applied by considering the same weight for the four investigated responses, e.g., the exponents r_p in Eqs. (4–(7) were set equal to 1 for all responses. However, the methodology can also be applied straightforwardly considering a different weight for the different responses. As mentioned above, increasing a certain exponent r_p has the effect of increasing the weight that the response p has in the determination of the optimal geometry. Decreasing it will make its influence to get lower. For instance, the designer can assign a higher importance to the minimization of the lateral displacement and the structural weight, while assigning a lower weight to the minimization of the torsional rotation and construction complexity. As an extreme case, if a certain exponent r_p is set to 0, the response p turns out not to affect the selection of the optimal geometry at all. We believe that this feature of the desirability function can be extremely important for the purpose of pattern optimization, since it allows a large freedom to the designer. Not only multiple responses can be properly defined for the purpose of optimizing the structure, but they can also be considered with a different impact.

To summarize, the main advantages of this methodology rely in its ease of application, its straightforwardness in providing the results and interpreting their reliability, and the capability to provide the optimal solution considering an almost unlimited number of responses, whose impact on the optimization process can be further modulated through the parameters r_p.

On the other hand, the weakest side of this desirability-based approach mainly relies on its dependence on the population of the defined solutions. As can easily be assessed by looking at Equations (2) and (4-7), this methodology assigns desirability values by comparing the performance of each solution i to the performance of all other solutions in the population P. As a result, the desirability of a certain pattern turns out to depend on the population in which it is included and analyzed. Consequently, the solution that is the most desirable within a certain population might not be the best one if the population is modified. A theoretically simple solution to this problem would be to define the individual desirability scores and the complexity index in a different way, so that they are independent of the population. This will require additional investigations.

Finally, it is worthy to mention that the desirability function approach can be applied to all the situations where a multi-response optimization is needed, and not only in the field of tall buildings for diagrid pattern optimization. It can be applied to other building types, as well as to an almost unlimited range of structural, architectural, and energetic systems. Its straightforwardness is expected to provide a useful tool to designers for the achievement of optimal solutions.

Author statement for the manuscript

“Selection of the optimal diagrid patterns in tall buildings within a multi-response framework: Application of the desirability function”.

by Domenico Scaramozzino, Bonierose Albitos, Giuseppe Lacidogna, and Alberto Carpinteri

All persons who meet authorship criteria are listed as authors, and all authors certify that they have participated sufficiently in the work to take public responsibility for the content, including participation in the concept, design, analysis, writing, or revision of the manuscript. Furthermore, each author certifies that this material or similar material has not been and will not be submitted to or published in any other publication before its appearance in the Journal of Building Engineering.

As reported in the Acknowledgments of the manuscript, this work mainly arises from the research activities carried out by Eng. Bonierose Albitos during her M.Sc. Thesis in Civil Engineering at Politecnico di Torino in 2021, under the supervision of Dr. Domenico Scaramozzino, Prof. Giuseppe Lacidogna and Prof. Alberto Carpinteri.

Author contributions:

- Conception and design of the study: Domenico Scaramozzino, Bonierose Albitos, Giuseppe Lacidogna, Alberto Carpinteri.
- Acquisition of data: Bonierose Albitos, Domenico Scaramozzino.
- Analysis and/or interpretation of data: Bonierose Albitos, Domenico Scaramozzino.
- First drafting of the manuscript: Domenico Scaramozzino.
- Revising the manuscript critically for important intellectual content: Domenico Scaramozzino, Bonierose Albitos, Giuseppe Lacidogna, Alberto Carpinteri.
- Approval of the version of the manuscript to be published: Domenico Scaramozzino, Bonierose Albitos, Giuseppe Lacidogna, Alberto Carpinteri.

All the authors agree to the current version of the manuscript to be published into the Journal of Building Engineering.

Declaration of competing interest

The authors declare that they have no known competing financial interests or personal relationships that could have appeared to influence the work reported in this paper.

Acknowledgments

The content presented in this paper arises from the MSc Thesis in Civil Engineering of Eng. Bonierose Albitos, graduated at the Politecnico di Torino under the supervision of Dr. Domenico Scaramozzino, Prof. Giuseppe Lacidogna and Prof. Alberto Carpinteri.

Appendix A. Supplementary data

Supplementary data to this article can be found online at https://doi.org/10.1016/j.jobe.2022.104645.

References

[1] M.M. Ali, K. Al-Kodmany, Tall buildings and urban habitat of the 21st century: a global perspective, Buildings 2 (2012) 384–423, https://doi.org/10.3390/buildings2040384.
[2] M.M. Ali, K.S. Moon, Structural developments in tall buildings: current trends and future prospects, Architect. Sci. Rev. 50 (2007) 205–223, https://doi.org/10.3763/asre.2007.5027.
[3] M.M. Ali, K.S. Moon, Advances in structural systems for tall buildings: emerging developments for contemporary urban giants, Buildings 8 (2018) 104, https://doi.org/10.3390/buildings8080104.
[4] M. Wang, X.-L. Du, F.-F. Sun, S. Nagarajaiah, Y.-W. Li, Fragility analysis and inelastic seismic performance of steel braced-core-tube frame outrigger tall buildings with passive adaptive negative stiffness damped outrigger, J. Build. Eng. 52 (2022), 104428, https://doi.org/10.1016/j.jobe.2022.104428.
[5] Q. Cao, J. Huang, L. Zhao, Z. Fang, Z. Zhang, Research on shear performance of corrugated steel plate shear walls with inelastic buckling of infilled plates under lateral loads, J. Build. Eng. 52 (2022), 104406, https://doi.org/10.1016/j.jobe.2022.104406.
[6] J. Li, Z. Wang, F. Li, B. Mou, T. Wang, Experimental and numerical study on the seismic performance of an L-shaped double-steel plate composite shear wall, J. Build. Eng. 49 (2022), https://doi.org/10.1016/j.jobe.2022.104015.
[7] J.K. Tan, X.H. Zhou, X. Nie, Y.H. Wang, K. Wang, Experimental and numerical investigation of cross-shaped buckling-restrained SPSWs with composite structure, J. Build. Eng. 47 (2022), https://doi.org/10.1016/j.jobe.2021.103873.
[8] K. Wang, M.N. Su, Y.H. Wang, J.K. Tan, H. bin Zhang, J. Guo, Behaviour of buckling-restrained steel plate shear wall with concrete-filled L-shaped built-up section tube composite frame, J. Build. Eng. 50 (2022), https://doi.org/10.1016/j.jobe.2022.104217.
[9] N. Labrecque, S. Ménard, M. Oudjene, P. Blanchet, Finite element study of hyperstructure systems with modular light-frame construction in high-rise buildings, Buildings 12 (2022), https://doi.org/10.3390/buildings12030330.
[10] C.P.D. Amoussou, H. Lei, Y. Halabi, W. Alhaddad, Performance-based seismic design methodology for tall buildings with outrigger and ladder systems, Structures 34 (2021) 2288–2307, https://doi.org/10.1016/j.istruc.2021.08.078.
[11] Z. Wang, K.D. Tsavdaridis, Optimality criteria-based minimum-weight design method for modular building systems subjected to generalised stiffness constraints: a comparative study, Eng. Struct. 251 (2022), https://doi.org/10.1016/j.engstruct.2021.113472.
[12] A. Xu, H. Lin, J. Fu, W. Sun, Wind-resistant structural optimization of supertall buildings based on high-frequency force balance wind tunnel experiment, Eng. Struct. 248 (2021), https://doi.org/10.1016/j.engstruct.2021.113247.
[13] M.R. Maqhareh, The evolutionary process of diagrid structure towards architectural, structural and sustainability concepts: reviewing case studies, J. Architect. Eng. Technol. 3 (2014) 121, https://doi.org/10.4172/2168-9717.1000121.
[14] E. Mele, Diagrid: the renaissance of steel structures for tall buildings geometry, design, behavior, Ce/Papers 1 (2017) 4437–4446, https://doi.org/10.1002/cepa.503.
[15] D. Scaramozzino, G. Lacidogna, Diagrid and hexagrid structures: new perspectives in design of tall buildings, Open Construct. Build Technol. J. 15 (2021) 214–217, https://doi.org/10.2174/1874836802115010.
[16] E. Asadi, H. Adeli, Diagrid: an innovative, sustainable, and efficient structural system, Struct. Des. Tall Special Build. 26 (2017) e1358, https://doi.org/10.1002/tal.1358.
[17] C. Liu, Q. Li, Z. Lu, H. Wu, A review of the diagrid structural system for tall buildings, Struct. Des. Tall Special Build. 27 (2018) 1–10, https://doi.org/10.1002/tal.1445.
[18] D. Scaramozzino, G. Lacidogna, A. Carpinteri, New trends towards enhanced structural efficiency and aesthetic potential in tall buildings: the case of diagrids, Appl. Sci. 10 (2020) 3917, https://doi.org/10.3390/APP10113917.
[19] K.S. Moon, J.J. Connor, J.E. Fernandez, Diagrid structural systems for tall buildings: characteristics and methodology for preliminary design, Struct. Des. Tall Special Build. 16 (2007) 205–230, https://doi.org/10.1002/tal.311.
[20] C. Zhang, F. Zhao, Y. Liu, Diagrid tube structures composed of straight diagonals with gradually varying angles, Struct. Des. Tall Special Build. 21 (2012) 283–295, https://doi.org/10.1002/tal.596.
[21] F. Zhao, C. Zhang, Diagonal arrangements of diagrid tube structures for preliminary design, Struct. Des. Tall Special Build. 24 (2015) 159–175.
[22] G.M. Montuori, E. Mele, G. Brandonisio, A. De Luca, Design criteria for diagrid tall buildings: stiffness versus strength, Struct. Des. Tall Special Build. (2014), https://doi.org/10.1002/tal.1144.
[23] E. Mele, M. Toreno, G. Brandonisio, A. De Luca, Diagrid structures for tall buildings: case studies and design considerations, Struct. Des. Tall Special Build. 23 (2014) 124–145, https://doi.org/10.1002/tal.1029.

[24] E. Mele, M. Imbimbo, V. Tomei, The effect of slenderness on the design of diagrid structures, Int. J. High-Rise Build. 8 (2019) 83–94, https://doi.org/10.21022/IJHRB.2019.8.2.83.
[25] S. Song, C. Zhang, Lateral stiffness and preliminary design methodology of twisted diagrid tube structures, Struct. Des. Tall Special Build. 29 (2020) 1–16, https://doi.org/10.1002/tal.1809.
[26] C. Liu, K. Ma, Calculation model of the lateral stiffness of high-rise diagrid tube structures based on the modular method, Struct. Des. Tall Special Build. 26 (2017) e1333, https://doi.org/10.1002/tal.1333.
[27] Q. Shi, F. Zhang, Simplified calculation of shear lag effect for high-rise diagrid tube structures, J. Build. Eng. 22 (2019) 486–495, https://doi.org/10.1016/j.jobe.2019.01.009.
[28] G. Lacidogna, D. Scaramozzino, A. Carpinteri, A matrix-based method for the structural analysis of diagrid systems, Eng. Struct. 193 (2019) 340–352, https://doi.org/10.1016/j.engstruct.2019.05.046.
[29] G. Lacidogna, D. Scaramozzino, A. Carpinteri, Influence of the geometrical shape on the structural behavior of diagrid tall buildings under lateral and torque actions, Develop. Built Environ. 2 (2020), 100009, https://doi.org/10.1016/j.dibe.2020.100009.
[30] G. Lacidogna, G. Nitti, D. Scaramozzino, A. Carpinteri, Diagrid systems coupled with closed- and open-section shear walls: optimization of geometrical characteristics in tall buildings, Procedia Manuf. (2020), 00.
[31] G. Lacidogna, G. Nitti, D. Scaramozzino, A. Carpinteri, Diagrid system coupled with shear walls: analytical investigation on the dynamical response in tall buildings, in: 8th ECCOMAS Thematic Conference on Computational Methods in Structural Dynamics and Earthquake Engineering, 2021, pp. 1793–1802.
[32] K.S. Moon, Optimal grid geometry of diagrid structures for tall buildings, Architect. Sci. Rev. 51 (2008) 239–251, https://doi.org/10.3763/asre.2008.5129.
[33] G.M. Montuori, E. Mele, G. Brandonisio, A. De Luca, Geometrical patterns for diagrid buildings: exploring alternative design strategies from the structural point of view, Eng. Struct. 71 (2014) 112–127, https://doi.org/10.1016/j.engstruct.2014.04.017.
[34] G. Angelucci, F. Mollaioli, Diagrid structural systems for tall buildings: changing pattern configuration through topological assessments, Struct. Des. Tall Special Build. (2017), e1396, https://doi.org/10.1002/tal.1396.
[35] V. Tomei, M. Imbimbo, E. Mele, Optimization of structural patterns for tall buildings: the case of diagrid, Eng. Struct. 171 (2018) 280–297, https://doi.org/10.1016/j.engstruct.2018.05.043.
[36] F. Cascone, D. Faiella, V. Tomei, E. Mele, Stress lines inspired structural patterns for tall buildings, Eng. Struct. 229 (2021), https://doi.org/10.1016/j.engstruct.2020.111546.
[37] F. Cascone, D. Faiella, V. Tomei, E. Mele, A structural grammar approach for the generative design of diagrid-like structures, Buildings 11 (2021) 1–21, https://doi.org/10.3390/buildings11030090.
[38] P. Ashtari, R. Karami, S. Farahmand-Tabar, Optimum geometrical pattern and design of real-size diagrid structures using accelerated fuzzy-genetic algorithm with bilinear membership function, Appl. Soft Comput. 110 (2021), https://doi.org/10.1016/j.asoc.2021.107646.
[39] T. Orhan, K. Taşkın, Automated topology design of high-rise diagrid buildings by genetic algorithm optimization, Struct. Des. Tall Special Build. 30 (2021) 1–29, https://doi.org/10.1002/tal.1853.
[40] A. Ardekani, I. Dabbaghchian, M. Alaghmandan, M. Golabchi, S.M. Hosseini, S.R. Mirghaderi, Parametric design of diagrid tall buildings regarding structural efficiency, Architect. Sci. Rev. 63 (2020) 87–102, https://doi.org/10.1080/00038628.2019.1704395.
[41] S. Mirniazmandan, M. Alaghmandan, F. Barazande, E. Rahimianzarif, Mutual effect of geometric modifications and diagrid structure on structural optimization of tall buildings, Architect. Sci. Rev. (2018), https://doi.org/10.1080/00038628.2018.1477043.
[42] L. Vera Candioti, M.M. De Zan, M.S. Camara, H.C. Goicoechea, Experimental design and multiple response optimization. Using the desirability function in analytical methods development, Talanta 124 (2014) 123–138.
[43] E.C. Harrington, The desirability function, Ind. Qual. Contr. 4 (1965) 494–498.
[44] G.C. Derringer, R. Suich, Simultaneous optimization of several response variables, J. Qual. Technol. 12 (1980) 214–219.
[45] G. Lacidogna, D. Scaramozzino, A. Carpinteri, Optimization of diagrid geometry based on the desirability function approach, Curved Layer. Struct. 7 (2020) 139–152, https://doi.org/10.1515/cls-2020-0011.
[46] American Society of Civil Engineers, ASCE 7-10. Minimum Design Loads for Buildings and Other Structures, 2010.
[47] Profile Library Checked Sections - Scia Engineer, 2010.
[48] K.S. Moon, Sustainable structural engineering strategies for tall buildings, Struct. Des. Tall Special Build. 17 (2008) 895–914, https://doi.org/10.1002/tal.475.